CANCER IMMUNOTHERAPY

10.1126/sciadv.1500845

The PTEN pathway in T_{regs} is a critical driver of the suppressive tumor microenvironment

Madhav D. Sharma,[1,2] Rahul Shinde,[1]* Tracy L. McGaha,[1,3]* Lei Huang,[1,4] Rikke B. Holmgaard,[5] Jedd D. Wolchok,[5] Mario R. Mautino,[6] Esteban Celis,[1,7] Arlene H. Sharpe,[8] Loise M. Francisco,[8] Jonathan D. Powell,[9] Hideo Yagita,[10] Andrew L. Mellor,[1,3] Bruce R. Blazar,[11] David H. Munn[1,2]†

The tumor microenvironment is profoundly immunosuppressive. We show that multiple tumor types create intratumoral immune suppression driven by a specialized form of regulatory T cell (T_{reg}) activation dependent on the PTEN (phosphatase and tensin homolog) lipid phosphatase. PTEN acted to stabilize T_{regs} in tumors, preventing them from reprogramming into inflammatory effector cells. In mice with a T_{reg}-specific deletion of PTEN, tumors grew slowly, were inflamed, and could not create an immunosuppressive tumor microenvironment. In normal mice, exposure to apoptotic tumor cells rapidly elicited PTEN-expressing T_{regs}, and PTEN-deficient mice were unable to maintain tolerance to apoptotic cells. In wild-type mice with large established tumors, pharmacologic inhibition of PTEN after chemotherapy or immunotherapy profoundly reconfigured the tumor microenvironment, changing it from a suppressive to an inflammatory milieu, and tumors underwent rapid regression. Thus, the immunosuppressive milieu in tumors must be actively maintained, and tumors become susceptible to immune attack if the PTEN pathway in T_{regs} is disrupted.

INTRODUCTION

Tumors are not invisible to the immune system (*1*–*4*). Analysis of patients' T cells suggests that many patients are chronically attempting to mount an immune response against their own tumors (*5*–*8*). However, in almost all cases, this attempted response is suppressed by potent inhibitory mechanisms within the tumor microenvironment. Multiple mechanisms contribute to this suppression (*9*), but one key component is the $Foxp3^+$ regulatory T cell (T_{reg}) system. Tumors actively recruit T_{regs}, and the T_{regs} in tumors become highly activated (*10*). If T_{regs} are transiently ablated in tumor-bearing mice, then the immune system rapidly attempts to attack the tumor (*11*, *12*). However, in these models, complete depletion of T_{regs} leads to lethal autoimmunity, yet partial depletion of T_{regs} is not sufficient to reverse the suppressive milieu in the tumor (*13*). To date, it has not been possible to preferentially target the T_{regs} that are protecting the tumor.

To improve this selectivity, we asked whether tumors might preferentially depend on certain molecular pathways to activate T_{regs}. This activation step is a critical control point in T_{reg} biology, because even fully mature T_{regs} require specific activation signals to become functionally suppressive (*14*). These signals include engagement of the T cell antigen receptor (TCR) (*15*, *16*). However, antigen specificity alone does not confer selectivity for tumors, because many of the T_{regs} in tumors appear to recognize normal self-antigens (*17*). Besides antigen, T_{regs} also integrate a variety of modulating signals from the local microenvironment during activation (*18*). This can produce "tailored" forms of activation, with distinct patterns of transcription factors and functional activity (*19*). We hypothesized that the unique environment of tumors might preferentially elicit certain characteristic pathways of T_{reg} activation.

The lipid phosphatase PTEN (phosphatase and tensin homolog) has recently been identified as an important signaling pathway in T_{regs} (*20*, *21*). Targeted deletion of PTEN causes T_{reg} instability (*20*), leading to progressive conversion into proinflammatory effector cells (so-called ex-T_{regs}), and eventual lupus-like autoimmunity. However, the mechanism by which PTEN stabilizes T_{regs} and the role that this might play in tumor biology remain unknown. Here, we show that many T_{regs} in the tumor microenvironment constitutively express PTEN and rely on this pathway to maintain their suppressive function. PTEN signaling in T_{regs} is required for the immune system to suppress responses to apoptotic cells, including apoptotic tumor cells. If this PTEN pathway is interrupted, then tumors lose the ability to create their usual highly suppressive milieu. The T_{regs} in tumors are destabilized and reprogram into inflammatory effector cells, the tumor milieu becomes proinflammatory and immunogenic, and even large established tumors undergo rapid regression.

RESULTS

Connection between IDO, PD-1, and PTEN in T_{regs}

Melanoma tumors in mice contained a large population of activated T_{regs} expressing the cell surface receptor programmed cell death-1 (PD-1) (Fig. 1A and fig. S1). PD-1 is a marker for activated T_{regs} in tumors (*10*), although its functional role remains unknown. The same $PD\text{-}1^+$ T_{regs} also coexpressed high levels of the Foxp3 binding partner Eos (*Ikzf4*),

[1]Cancer Center, Georgia Regents University, Augusta, GA 30912, USA. [2]Department of Pediatrics, Medical College of Georgia, Georgia Regents University, Augusta, GA 30912, USA. [3]Department of Medicine, Medical College of Georgia, Georgia Regents University, Augusta, GA 30912, USA. [4]Department of Radiology, Medical College of Georgia, Georgia Regents University, Augusta, GA 30912, USA. [5]Department of Medicine, Immunology Program and Ludwig Center, Memorial Sloan Kettering Cancer Center; Weill Cornell Medical School and Graduate School of Biomedical Sciences; and Ludwig Institute for Cancer Research, New York, NY 10065, USA. [6]NewLink Genetics Inc., Ames, IA 50010, USA. [7]Department of Biochemistry, Medical College of Georgia, Georgia Regents University, Augusta, GA 30912, USA. [8]Department of Microbiology and Immunobiology, Harvard Medical School, Boston, MA 02115, USA. [9]Sidney Kimmel Comprehensive Cancer Research Center, Department of Oncology, Johns Hopkins University School of Medicine, Baltimore, MD 21231, USA. [10]Department of Immunology, Juntendo University School of Medicine, Bunkyo-ku, Tokyo 113-8421, Japan. [11]Division of Blood and Marrow Transplantation, Department of Pediatrics, University of Minnesota, Minneapolis, MN 55455, USA.
*Present address: Princess Margaret Cancer Centre, University Hospital Network, and Department of Immunology, University of Toronto, Toronto, Ontario M5G 2M9, Canada.
†Corresponding author. E-mail: dmunn@gru.edu

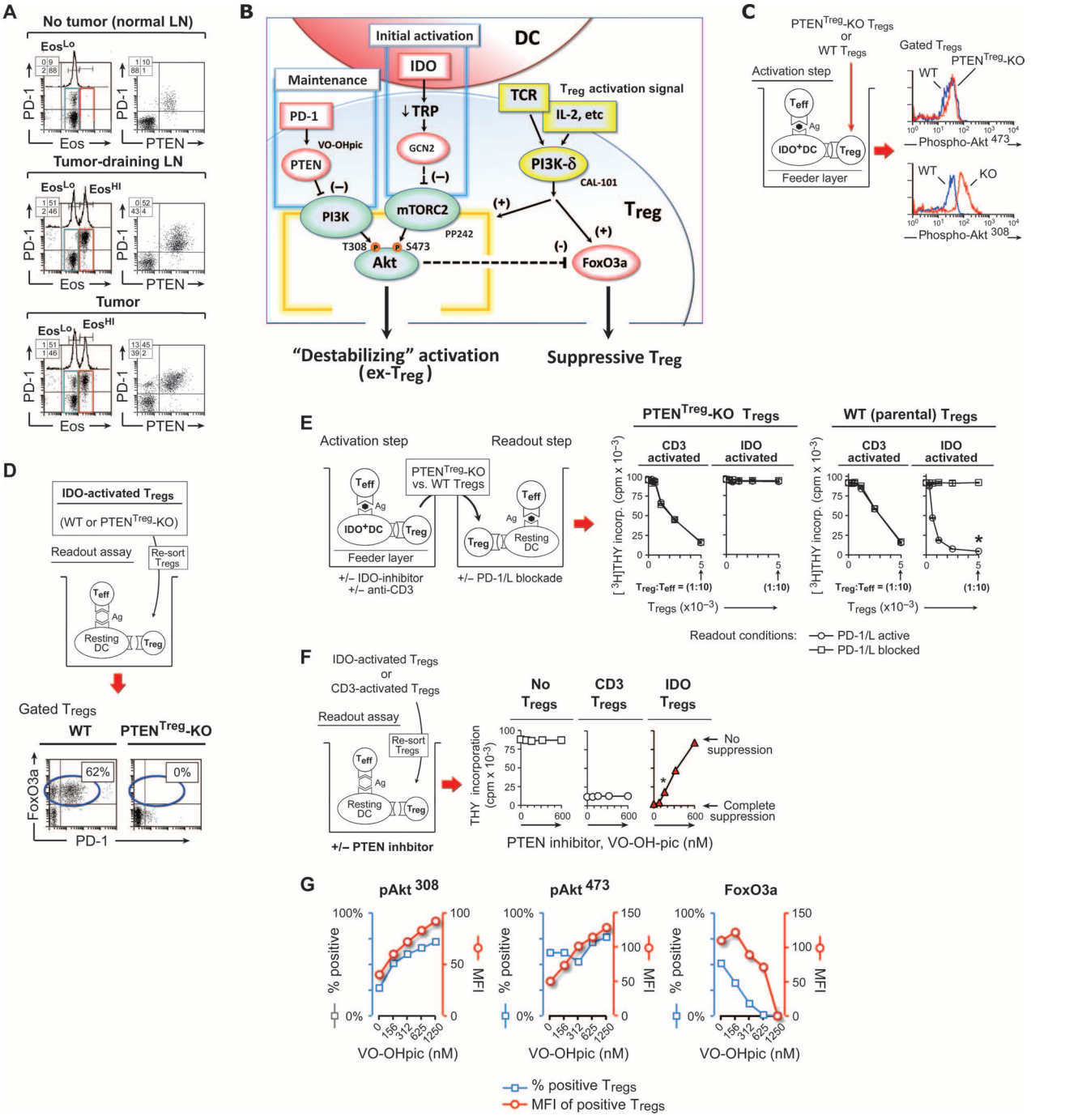

Fig. 1. PTEN is required to maintain IDO-induced T_{reg} activation. (**A**) Analysis of peripheral T_{regs} from LNs of normal mice without tumor or from TDLNs and tumor of mice with B16F10 tumors, gated on $CD4^+Foxp3^+$ T_{regs}. (**B**) Proposed model for regulation of Akt by IDO and the PD-1→PTEN pathway during T_{reg} activation, based on data from figs. S2 to S8. (**C** and **D**) T_{regs} from $PTEN^{Treg}$-KO mice or wild-type (WT) controls were activated in vitro for 2 days with IDO^+ DCs from TDLNs, using the coculture system described in fig. S2A. (C) T_{regs} were analyzed for phosphorylation of Akt by FACS at the end of activation. (D) After activation, T_{regs} were re-sorted and tested in readout assays for their ability to maintain FoxO3a and PD-1. (**E**) $PTEN^{Treg}$-KO T_{regs} or WT (parental) control T_{regs} were activated either with IDO^+ DCs from TDLNs or using conventional anti-CD3 mitogen with IDO blocked. After 2 days, T_{regs} were re-sorted and tested in readout assays for functional suppressor activity, as in fig. S2A. Each point is the mean of triplicate cocultures; error bars show SD (most are less than ±5%, smaller than the symbols). *$P < 0.01$ by analysis of variance (ANOVA) versus PD-1/L blockade (all other groups not significant versus PD-1/L blockade). (**F** and **G**) WT T_{regs} were activated with either IDO^+ TDLN DCs or conventional αCD3 mitogen and then sorted and tested for functional suppressor activity (F) in the presence of PTEN inhibitor VO-OHpic. Mean of triplicate cocultures; SD bars are smaller than the symbols; *$P < 0.01$ by ANOVA versus no VO-OHpic. (G) In parallel experiments, the re-sorted T_{regs} were recovered at the end of the suppression assay and assessed for their level of Akt phosphorylation and detectable FoxO3a expression by FACS. Panels are representative of three to five independent experiments each.

which can be up-regulated in tumors by the immunoregulatory enzyme indoleamine 2,3-dioxygenase (IDO), as we have shown (*22*). IDO promotes tolerance and immunosuppression in the immune system (*23*), and it can directly activate T_{regs} in tumors (*22*, *24*). These same PD-1^{+} Eos^{HI} T_{regs} also coexpressed PTEN phosphatase (Fig. 1A, right-hand panels).

To help elucidate the connection between IDO, PD-1, and PTEN in activated T_{regs}, we used the in vitro culture system shown in fig. S2. Resting T_{regs} were activated by coculture with IDO-expressing dendritic cells (DCs) and activated effector cells. After initial activation by IDO, the T_{regs} then became strictly dependent on PD-1 to maintain their functional activity (fig. S2A). We hypothesized that the IDO and PD-1 pathways might converge at the level of Akt kinase. In most T cells, high Akt signaling is required for normal activation; however, T_{regs} are unusual in that they must keep Akt signaling low during activation or else they will lose their suppressive phenotype (*25*). PD-1 is known to inhibit Akt via the activation of PTEN phosphatase (*26*, *27*), but the effect of IDO on Akt was unknown. We found that IDO inhibited phosphorylation of Akt on Ser^{473} (fig. S2B). Ser^{473} is the target of the mTOR TORC2 complex; consistent with this, pharmacologic inhibition of mTOR could fully substitute for IDO during T_{reg} activation (fig. S2C). In vivo, administration of an IDO inhibitor drug to tumor-bearing mice increased pAkt^{473} phosphorylation in T_{regs} (fig. S3). Thus, both IDO and PD-1 appeared to restrain excessive Akt signaling in activated T_{regs}.

The phosphorylation status of Akt is only a proxy marker and is very labile. We sought a more stable biomarker that might reflect the longer-term impact of dysregulated Akt signaling on the overall T_{reg} phenotype. The transcription factor FoxO3a is important in T_{reg} function (*28*), and it is sensitive to the activity of Akt (*29*–*31*). In the short term, phosphorylation by Akt drives nuclear exclusion of FoxO3a and blocks its function (*32*), but in the long term, overactivity of Akt leads to degradation of FoxO3a (*33*). Fluorescence-activated cell sorting (FACS) analysis of T_{regs} showed that FoxO3a expression was highly bimodal, with some T_{regs} expressing none and some having strongly positive expression (fig. S4). In vitro, after activation cocultures, the fraction of T_{regs} that became FoxO3a-positive tracked with the suppressor activity controlled by IDO and mTOR (fig. S5A), whereas on a cell-by-cell basis, those T_{regs} that expressed PD-1 also coexpressed FoxO3a (Fig. 5B). Functionally, T_{regs} from FoxO3-deficient mice (*28*) were selectively unable to mediate the form of suppressor activity created by the IDO and PD-1, even though conventional CD3-induced T_{reg} activity remained intact (fig. S5C). Thus, although FoxO3a itself was not unique or restricted only to IDO and PD-1 (*29*, *30*), we hypothesized that loss (down-regulation) of FoxO3a could be an informative biomarker for loss of the suppressive T_{reg} phenotype of interest.

IDO and PD-1 acted sequentially. IDO up-regulated expression of PD-1 on the T_{regs} via a process requiring tryptophan depletion and signaling via the amino acid–sensitive GCN2 kinase (*34*) (figs. S6 and S7, A to C). PD-1 was then required to maintain the IDO-induced activation state (fig. S8). If the PD-1 pathway was blocked, then Akt phosphorylation rapidly became high, FoxO3a was lost, and suppression activity was abrogated. On the basis of these findings, we hypothesized the model shown in Fig. 1B, in which IDO and PD-1 sequentially act to maintain the suppressive T_{reg} phenotype. The key implication of this model was that maintenance of the suppressive phenotype required continuous, ongoing control of Akt: If this control was disrupted, then the suppressive phenotype was rapidly lost. Thus, the critical leverage point for continued suppression became PD-1 signaling via PTEN.

Maintenance of the T_{reg} activation state by PTEN

PTEN is an important target for multiple upstream pathways, because it inhibits phosphatidylinositol 3-kinase (PI3K) and thus limits phosphorylation of Akt (*26*, *27*). In addition to PD-1, PTEN is also downstream of neuropilin-1, a potent activator of T_{regs} (*29*). To assess the role of PTEN, we crossed mice bearing a floxed PTEN allele (*35*) with Bac-transgenic mice expressing a Cre-GFP (green fluorescent protein) fusion protein under the Foxp3 promoter (*36*). This Cre strain deletes in ~95% of Foxp3^{+} T_{regs} (*36*). Consistent with this, our PTEN^{Treg}-KO mice expressed Cre-GFP in ~95% of Foxp3^{+} cells and showed no detectable PTEN expression in Foxp3^{+} T_{regs} from tumors or tumor-draining lymph nodes (TDLNs) (fig. S9). The phenotype of this particular Cre/lox intercross was somewhat less penetrant than other PTEN-deficient strains that have been described (*20*), in that our mice were healthy when young and did not develop spontaneous autoimmunity until later in life (which is an important advantage for tumor studies). However, even in our young, healthy PTEN^{Treg}-KO mice, the T_{regs} were unable to control phosphorylation of Akt at Thr^{308} during T_{reg} activation in vitro (Fig. 1C) and could not maintain the activated FoxO3a^{+} PD-1^{+} suppressive phenotype after re-sorting (Fig. 1, D and E). This was not due to a global defect in all T_{reg} activity, because conventional CD3-induced T_{reg} activity remained intact in these mice (Fig. 1E). Thus, the defect in PTEN^{Treg}-KO T_{regs} was a selective one, but—at least in the case of IDO—it profoundly compromised their ability to maintain the activated T_{reg} phenotype.

We next asked whether PTEN could be pharmacologically targeted. PTEN inhibitor drugs are under active preclinical investigation for their neuroprotective and cardioprotective effects; we tested VO-OHpic, a high-affinity small-molecule inhibitor of PTEN (*37*), for its ability to block suppression by IDO-activated T_{regs} in vitro (Fig. 1F). In the absence of any T_{regs}, VO-OHpic had no effect on the readout T cells (neither toxic nor stimulatory). When control CD3-activated T_{regs} were added, VO-OHpic had no effect on their ability to suppress. However, when the same T_{regs} were activated by IDO, VO-OHpic fully blocked their suppressor activity, in a dose-dependent fashion. This was accompanied by progressive increase in phosphorylation of Akt in the T_{regs} and progressive loss of detectable FoxO3a (Fig. 1G). (In these studies, Thr^{308} was the direct target of PTEN→PI3K, and there was no IDO in the system to inhibit phosphorylation of Ser^{473}; hence, both increased together as the T_{regs} became activated.)

Failure to create a suppressive tumor microenvironment in the absence of PTEN-T_{regs}

We next tested the effect of PTEN^{Treg}-KO hosts on tumor growth. Aggressive melanoma tumors implanted in PTEN^{Treg}-KO hosts grew much slower than the same tumors implanted in wild-type parental strains (Fig. 2A). Slower growth was also seen with E.G7 (EL4-OVA) and LLC tumors (fig. S10). Analysis of immune cells infiltrating the tumors (Fig. 2B) showed that wild-type hosts contained many PTEN^{+} T_{regs} that also coexpressed FoxO3a and PD-1, consistent with a suppressive phenotype. In contrast, the T_{regs} in PTEN^{Treg}-KO tumors did not express FoxO3a or PD-1; instead, they appeared unstable, with many expressing proinflammatory markers such as interleukin-2 (IL-2), CD40L, and IL-17 (Fig. 2B, lower panels, and fig. S11). All of these "reprogrammed" T_{regs} continued to express residual Foxp3 (Fig. 2B, bottom graph), thus showing that they were derived from former T_{regs}. The presence of these unstable, reprogrammed T_{regs} is consistent with our previous descriptions of T_{reg} reprogramming in tumors when IDO is blocked

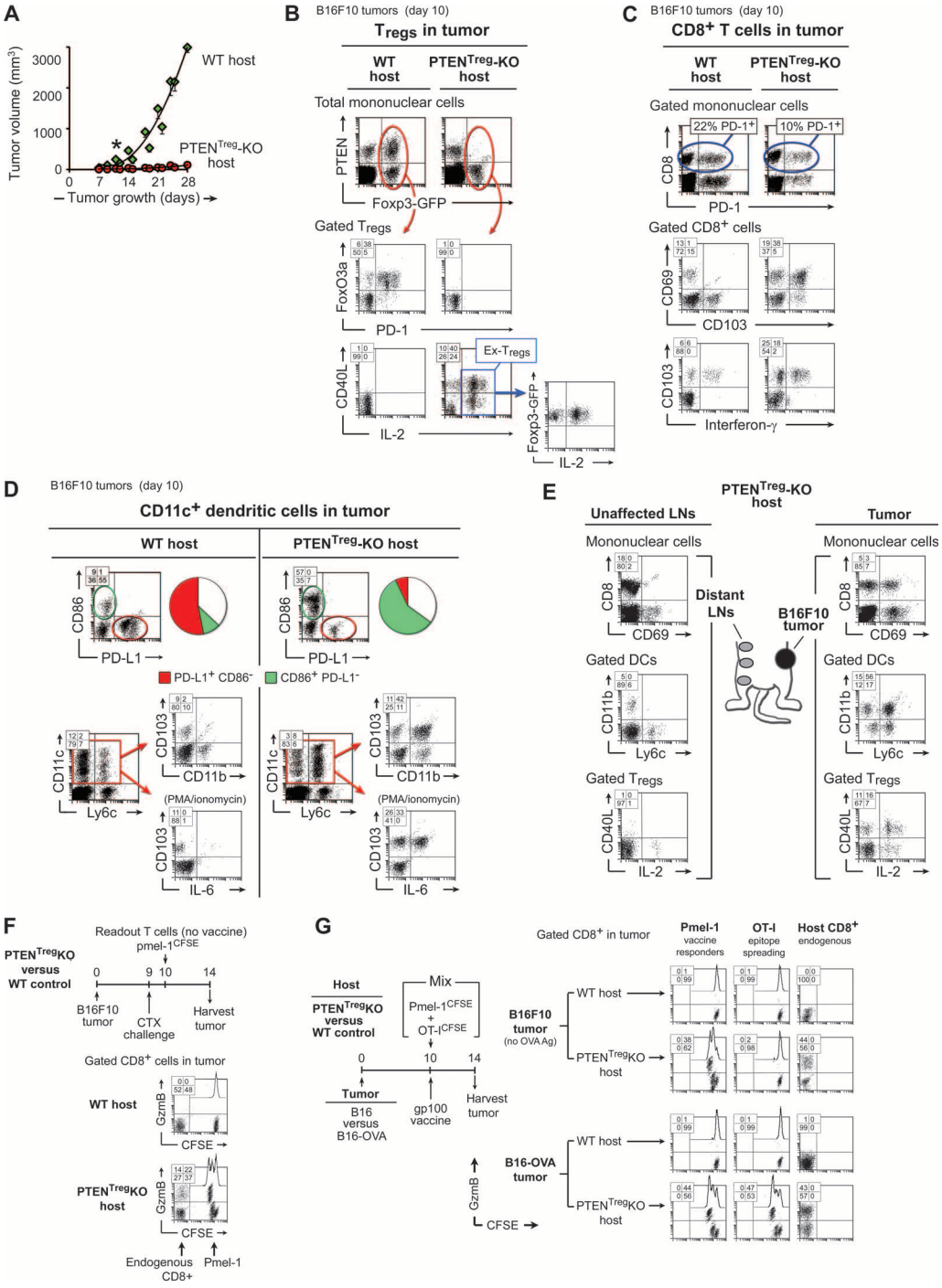

Fig. 2. Tumors in PTEN^{Treg}-KO hosts lose the ability to create a suppressive intratumoral milieu. (**A**) Growth of B16F10 tumors in PTEN^{Treg}-KO hosts and WT B6 hosts. Pooled data from four experiments, $n = 6$ to 8 tumors per time point. *$P < 0.05$ versus WT, and all points thereafter. (**B** to **D**) Analysis of tumor-infiltrating immune cells in B16F10 tumors after 10 days of tumor growth in either PTEN^{Treg}-KO or parental Foxp3-GFP-Cre hosts: (B) T_{regs}, (C) CD8$^+$ T cells, and (D) CD11c$^+$ DCs. Representative of a total of nine experiments on days 10, 15, and 22. Intracellular cytokines were measured after 4 hours of activation with phorbol 12-myristate 13-acetate (PMA)/ionomycin. (**E**) Tumors were implanted on one side of PTEN^{Treg}-KO hosts; then, on day 14, the phenotype of T cells and DCs within the tumor was compared with pooled contralateral LNs, distant from the tumor. (**F**) Carboxyfluorescein diacetate succinimidyl ester (CFSE)–labeled pmel-1 cells, recognizing tumor-associated gp100, were transferred into WT or PTEN^{Treg}-KO hosts after a single dose of cyclophosphamide (CTX) to release tumor antigens. (**G**) PTEN^{Treg}-KO hosts or WT controls were implanted with B16F10 tumors or B16-OVA tumors bearing a nominal antigen. Mice then received a mixture of two CFSE-labeled responder cells: pmel-1 recognizing gp100 and OT-I recognizing OVA. Mice were then vaccinated against only the gp100 antigen, and tumors were analyzed 4 days later for evidence of epitope spreading (OT-I activation). (E) to (G) are representative of at least three experiments each.

(*22*, *38*). Similar unstable ex-T_{regs} have been described during autoimmunity in mice with targeted deletion of PTEN in T_{regs} (*20*).

The tumor-infiltrating $CD8^+$ T cells in $PTEN^{Treg}$-KO hosts appeared more activated (Fig. 2C). Fewer $CD8^+$ cells were $PD\text{-}1^+$ (implying an "exhausted" phenotype) and more had an activated phenotype expressing $CD103^+$, $CD69^+$, and interferon-γ (IFN-γ). DCs in tumors from $PTEN^{Treg}$-KO mice also showed a more activated phenotype (Fig. 2D). More DCs expressed an activated myeloid DC phenotype of $Ly6c^+CD11b^+CD103^+$, which has been associated with antitumor immune surveillance (*39*). Many of these $CD103^+$ DCs produced IL-6 (bottom panels). This was significant because, as we will show, IL-6 proved to be a key driver of T_{reg} reprogramming. Similar changes were seen when E.G7 lymphoma tumors were grown in $PTEN^{Treg}$-KO hosts (fig. S12).

These inflammatory changes were physically localized only to the tumor and TDLNs (Fig. 2E). Elsewhere in these (young, healthy) $PTEN^{Treg}$-KO hosts, the T cells and DCs appeared normal. This was informative, because it showed that the tumor became a potent local stimulus for inflammation when the host lacked the PTEN-T_{reg} pathway.

In $PTEN^{Treg}$-KO hosts, antigen-specific $CD8^+$ T cells became aware of tumor-associated antigens after chemotherapy. Mice with established B16F10 tumors were treated with a single dose of CTX to release tumor antigens and then received a CFSE-labeled cohort of resting pmel-1 T cells, reactive with a tumor-associated gp100 antigen. In $PTEN^{Treg}$-KO hosts, the resting pmel-1 cells became activated and proliferated in tumors, whereas proliferation was suppressed in wild-type hosts (Fig. 2F). Similarly, when tumor-bearing mice were treated with T cell adoptive transfer and antitumor vaccination, $PTEN^{Treg}$-KO hosts supported generalization of the immune response to new, additional T cells, recognizing antigen derived only from the tumor (Fig. 2G). No such epitope spreading occurred in wild-type hosts. (In all of these studies, the readout T cells were purified by negative selection, because this was important to prevent artifactual activation, as shown in fig. S13.) Thus, taken together, in $PTEN^{Treg}$-KO hosts, tumors were unable to create their usual suppressive tumor microenvironment and instead were regarded by the immune system as spontaneously inflammatory and immunogenic.

Reconfiguration of the suppressive microenvironment in established tumors

We next asked whether a similar antitumor inflammatory response could be induced in wild-type mice by pharmacologic inhibition of PTEN. This was a more demanding setting because the tumor had already established a suppressive milieu. Administering PTEN inhibitor by itself had no effect on growth of established tumors; however, if mice also received immunotherapy (vaccine plus pmel-1 T cells), then blocking PTEN had a potent effect, allowing rapid regression of tumors (Fig. 3A). Similar results were seen with ovalbumin (OVA)–expressing EL4 tumors and anti-OVA vaccine (Fig. 3B).

Analysis of treated tumors revealed that phosphorylation of Akt in T_{regs} remained low when tumors received only vaccine/T cells alone, but Akt phosphorylation became high when the PTEN inhibitor was added (Fig. 3C, red histograms). Phosphorylation was increased at both Thr^{308} and Ser^{473} sites. This is the expected pattern during activation of conventional (non-T_{reg}) $CD4^+$ cells (*40*), but it should not occur in T_{regs}, which need to keep Akt activity low. Thus, blocking PTEN caused dysregulated control of Akt in T_{regs}. (Notably, the T_{regs} were analyzed after 4 days of treatment; thus, Akt phosphorylation reflected the whole process of activation and destabilization, over and above the direct effects of the PTEN inhibitor on Thr^{308}.)

Consistent with their inability to control Akt activity, intratumoral T_{regs} in $PTEN^{Treg}$-KO mice lost detectable FoxO3a and PD-1 (Fig. 3C, dot plots). They also became destabilized and up-regulated proinflammatory IL-2 and CD40L (that is, underwent reprogramming). As a biologic control for these effects, we included the PI3K-δ inhibitor CAL-101 (*41*), which inhibits T_{reg} activity but does not affect PTEN. When tested in our in vitro model, CAL-101 inhibited T_{reg} activation as expected, but it was not selective, inhibiting both IDO-induced and CD3-induced suppression (fig. S14). In vivo, CAL-101 did not increase Akt phosphorylation in T_{regs}, did not cause loss of FoxO3a and PD-1, and did not drive T_{reg} destabilization and reprogramming (Fig. 3C). In our previous studies of T_{reg} reprogramming, we had shown that TCR-mediated activation is strictly required for reprogramming to occur (*22*, *38*, *42*). Thus, CAL-101 appeared to inhibit all T_{reg} activation (*41*), including the "destabilizing" activation that was required to drive reprogramming, whereas VO-OHpic allowed activation, but in a destabilizing fashion.

Further characterization of the tumor milieu after VO-OHpic treatment showed that vaccine-specific OT-I cells were suppressed when PTEN was active but were able to proliferate and up-regulate granzyme B when PTEN was blocked (Fig. 3D). Tumors also contained more activated, proinflammatory $Ly6c^+CD11b^+$ myeloid DCs when PTEN was blocked, and the DCs expressed more CD86 and less PD-L1 (Fig. 3D, lower panels). The contribution of the immunotherapy regimen (T cells and vaccine) was important, because successful transformation of the tumor microenvironment required both vaccine-activated T cells and inhibition of PTEN (Fig. 3E).

Finally, we noted that the PTEN inhibitor itself had no effect on a normal vaccine response in the absence of tumor (fig. S15A). The same was true for genetic ablation of PTEN (fig. S15B): In the absence of a suppressive tumor, ablating PTEN had no effect on the response to vaccine. Thus, the effect of PTEN inhibition was to reverse the specific tumor-induced suppression, rather than to nonspecifically augment all immune responses.

PTEN-T_{regs} and tolerance to apoptotic cells

$PTEN^+$ T_{regs} were crucial for tumors, but it was not clear what role these cells normally played in the immune system. Other strains of mice with T_{reg}-specific deletion of PTEN develop a spontaneous lupus-like autoimmunity as they age (*20*). Such "lupus-prone" phenotypes can reflect an inability to maintain tolerance to apoptotic cells (*43*). We have previously shown that apoptotic cells are potent inducers of IDO, and IDO-deficient mice fail to create tolerance to apoptotic cells and instead develop lupus autoimmunity (*23*). We triggered apoptosis in EL4 tumor cells by in vitro treatment with staurosporine for 4 hours, and then injected the apoptotic tumor cells into normal, tumor-free mice. Apoptotic tumor cells drove extensive up-regulation of IDO in draining LNs (DLNs) (Fig. 4A). This IDO expression was functionally important, because mice treated with an IDO inhibitor became responsive to antigen from the apoptotic cells, whereas responses were suppressed if IDO was active (Fig. 4B). Apoptotic tumor cells elicited a prominent population of $PTEN^+$ T_{regs} expressing $FoxO3a^+$ and $PD\text{-}1^+$ in local DLNs, and induction of these T_{regs} was blocked by the IDO inhibitor (Fig. 4C). When T_{regs} were sorted from DLNs after challenge with apoptotic cells, these T_{regs} mediated potent, spontaneous suppression ex vivo, in the PD-1–dependent fashion characteristic of IDO-induced activation (Fig. 4D). In contrast, T_{regs} from resting LNs

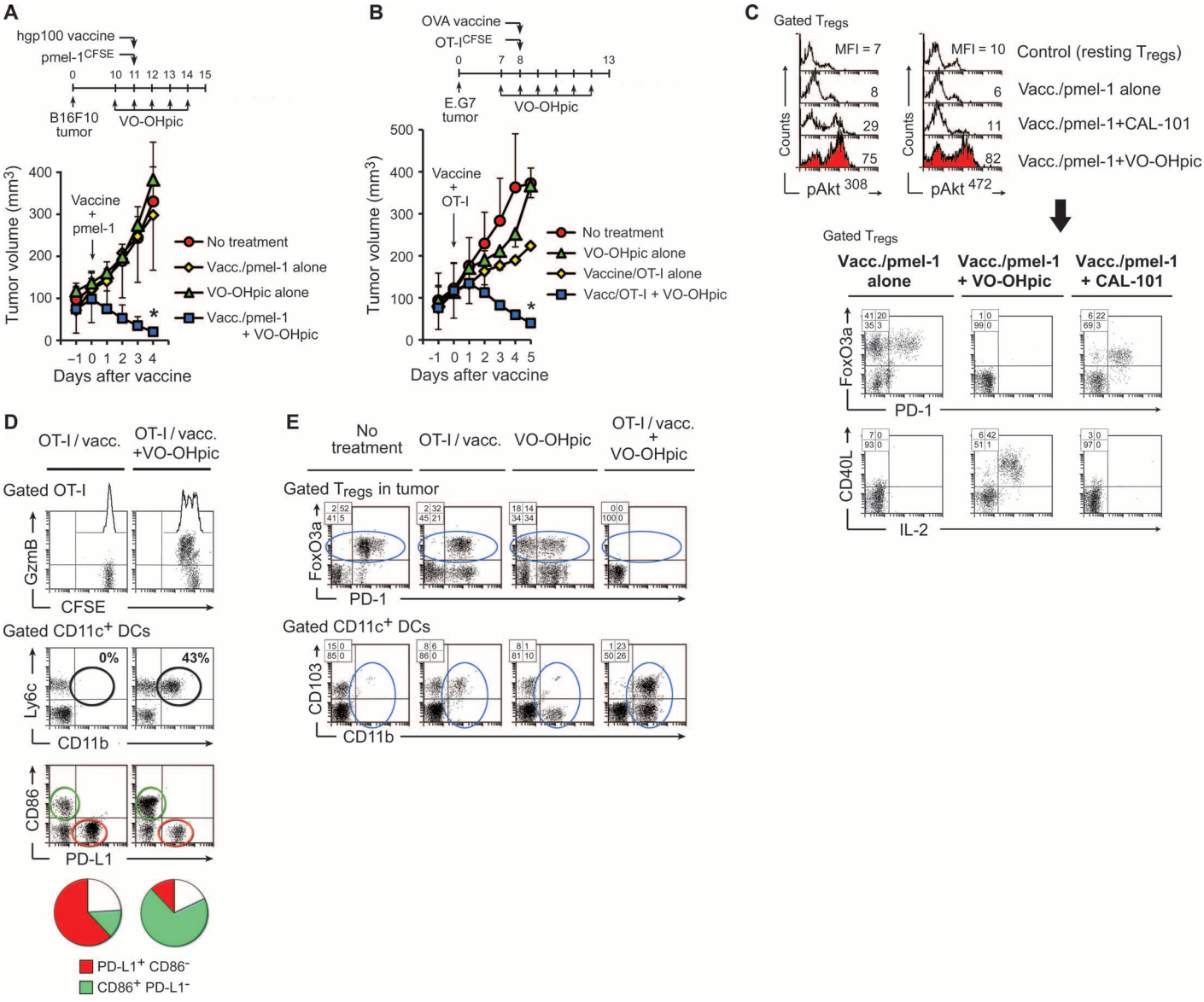

Fig. 3. Vaccination drives rapid reconfiguration of the suppressive tumor microenvironment when PTEN is blocked. (**A** and **B**) WT C57Bl/6 mice with established B16F10 tumors (A) or E.G7 tumors (B) were treated with tumor-specific T cells (pmel-1 or OT-I) plus cognate vaccine, with or without VO-OHpic [10 mg kg^{-1} day^{-1} intraperitoneally (ip)] as indicated. Each curve represents pooled data from a total of 6 to 22 tumors in three to five independent experiments, measured serially. *$P < 0.01$ versus all other curves by ANOVA. (**C**) B16F10 tumors received vaccine and pmel-1 cells as in (A), with or without either VO-OHpic or CAL-101 (PI3K-δ inhibitor, 30 mg kg^{-1} day^{-1} ip). Tumors were harvested 4 days after vaccine and stained for Akt phosphorylation in gated GFP^+ T_{regs} and for evidence of T_{reg} destabilization and reprogramming. Representative of five experiments. (**D**) Effect of VO-OHpic on intratumoral OT-I responses and activation of tumor-associated DCs in mice with E.G7 tumors, treated with OT-I/vaccine as in (B), with or without VO-OHpic. Similar results were seen using B16F10 with pmel-1/hgp100 vaccine. (**E**) Requirement for both VO-OHpic and activated OT-I/vaccine to successfully drive T_{reg} destabilization and DC activation in established E.G7 tumors. (D) and (E) are representative of at least three experiments each.

showed no spontaneous suppressor activity. [Readout assays in these experiments were driven by cognate antigen, with no CD3 mitogen, and under these conditions, resting T_{regs} do not show spontaneous suppression (*14*).] Thus, apoptotic tumor cells appeared to directly elicit the IDO-induced, PD-1–dependent $PTEN^+$ $FoxO3a^+$ $PD\text{-}1^+$ form of T_{reg} activation.

To test whether these T_{regs} were mechanistically controlled by PTEN, we treated mice with the PTEN inhibitor during exposure to apoptotic cells, and we compared wild-type hosts to $PTEN^{Treg}$-KO hosts (Fig. 4E). When wild-type mice received VO-OHpic at the time of challenge, apoptotic cells elicited no $FoxO3a^+PD\text{-}1^+$ T_{regs} (Fig. 4E, top row). Instead, the apoptotic cells now induced inflammatory $CD11b^+CD103^+$ myeloid DCs, and the readout OT-I T cells were able to respond to antigens from apoptotic cells (lower rows). Similar results were seen when genetically defined $PTEN^{Treg}$-KO mice were challenged with apoptotic cells (Fig. 4E, right-hand plots). In these $PTEN^{Treg}$-KO mice,

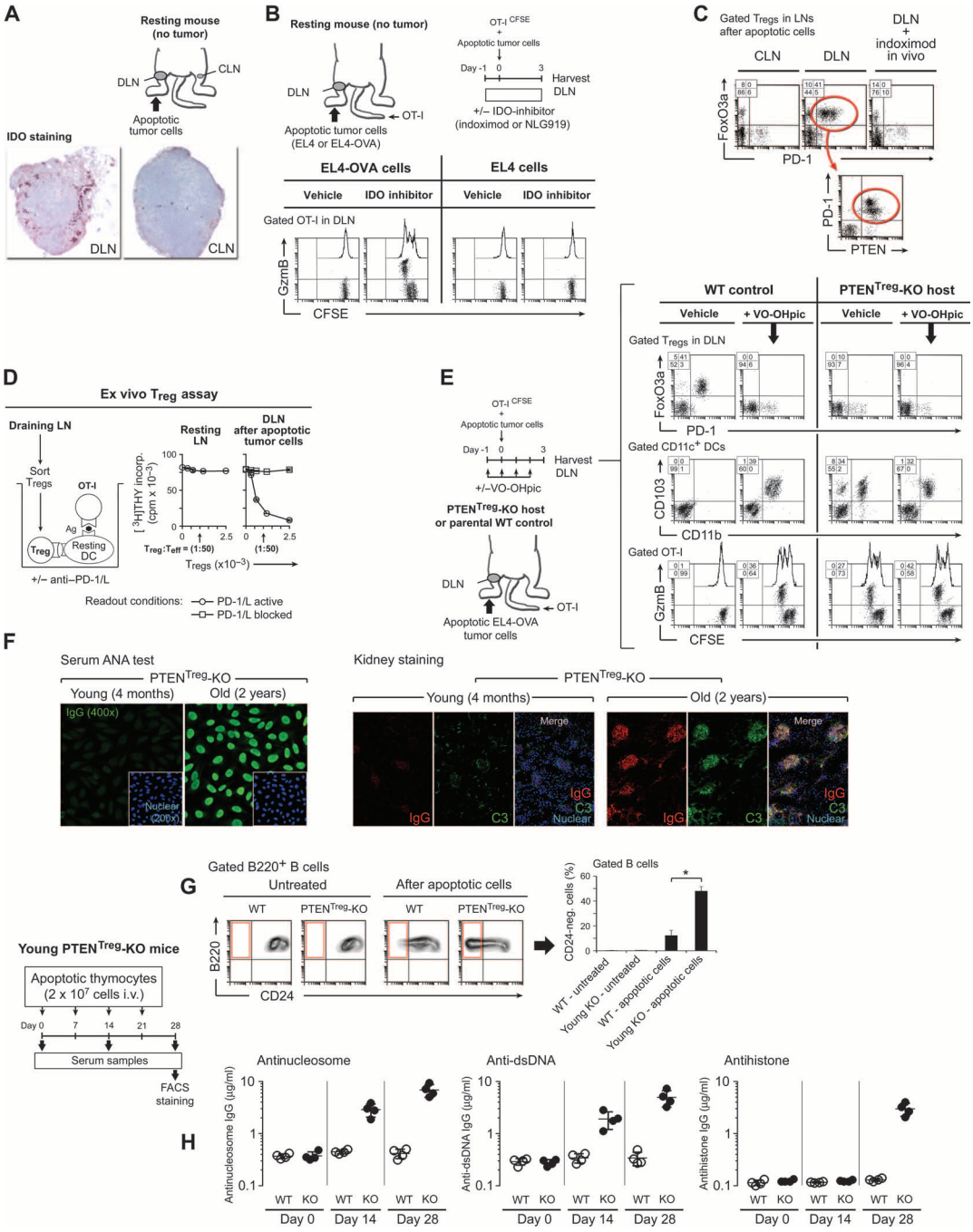

Fig. 4. The PTEN pathway in T_{regs} is required to suppress immune responses to apoptotic cells. (**A** to **D**) Normal mice without tumors received footpad injection of dying EL4 tumor cells (treated for 3 hours in vitro with staurosporine to induce apoptosis). (A) After 48 hours, DLNs and unaffected contralateral LNs (CLNs) were stained for IDO (red chromogen). (B) OT-I response to cell-associated antigen from apoptotic EL4-OVA (E.G7) cells, or parental EL4 controls, with or without treatment in vivo with the IDO inhibitor drug in drinking water. (C) After apoptotic cell injection, Foxp3$^+$ T_{regs} were compared in DLNs versus control distant CLNs for activation of PTEN-T_{regs}, with or without IDO inhibitor (indoximod). (D) Two days after challenge with apoptotic cells, T_{regs} were sorted from DLNs (or control LNs without injection) and directly tested ex vivo for constitutive suppressor activity, as described in fig. S2A, with or without PD-1/L blockade in the readout assay. Each point is the mean of triplicate cocultures; bars show SD (all are less than ±5%, smaller than the symbols). (**E**) Effect of PTEN inhibitor (VO-OHpic) on the immune response to apoptotic EL4-OVA cells (E.G7). Responses were compared in WT (parental) hosts and PTEN^{Treg}-KO hosts, with and without VO-OHpic. (**F**) Old mice (1- to 2-year-old retired breeders) and young mice (<6 months) from the PTEN^{Treg}-KO strain were tested for spontaneous antinuclear autoantibodies in serum (ANA, left) and deposition of immunoglobulin G (IgG) and complement C3 in the kidney (right). (**G** and **H**) Young, healthy PTEN^{Treg}-KO mice, or control WT B6 mice, were challenged with 2 × 10^7 apoptotic thymocytes weekly for four doses intravenously. Splenic B cells were analyzed for CD24 expression on day 28 (G). Serum titers of autoantibodies were compared at days 0, 14, and 28 (H). Pooled data from four to five mice; bars show SD.

there was no additional effect of adding VO-OHpic, suggesting that the PTEN expressed in T_{regs} was an important target of VO-OHpic in this model.

On the basis of the response to apoptotic tumor cells, we asked whether the PTEN^{Treg}-KO mice had a generalized defect in tolerance to all apoptotic cells. Although the mice in our strain were healthy when young, some of the older mice (>1 year) spontaneously developed antinuclear antibody and immune complex deposition in the kidney, consistent with lupus-like autoimmunity (Fig. 4F). Therefore, to test the younger, asymptomatic PTEN^{Treg}-KO mice for an underlying defect in tolerance, we challenged them with intravenous injection of apoptotic thymocytes. These were syngeneic cells, and wild-type mice were fully tolerant to them; however, the PTEN^{Treg}-KO mice showed widespread B cell activation (assessed as loss of CD24, Fig. 4G) and rapidly developed multiple autoantibodies against classic apoptotic cell antigens (nucleosome, double-stranded DNA, and histone; Fig. 4H). Thus, when confronted with large numbers of apoptotic cells, the PTEN pathway in T_{regs} appeared critical for the host to create immune suppression and tolerance.

Synergy between chemotherapy and PTEN inhibition

Chemotherapy releases a wave of dying tumor cells. We hypothesized that the tumor might become critically dependent on the PTEN pathway after chemotherapy. Mice bearing established B16F10 tumors received a single injection of CTX, with or without VO-OHpic (Fig. 5A). The dose of CTX was modest and by itself had no effect on these resistant tumors. VO-OHpic alone also had no effect on tumor growth. However, together these agents displayed striking synergy, causing rapid shrinkage of the tumor within 4 to 5 days. Mice received no other immunotherapy or T cell transfer; hence, any immunologic effects were the spontaneous contribution of the host immune system. Chemotherapy plus VO-OHpic was well tolerated, without weight loss or other obvious toxicity. In validation studies, mice without tumors were treated with VO-OHpic for up to 21 days and did not develop detectable autoantibodies (fig. S16).

In this chemotherapy model, inhibiting PTEN caused much more potent synergy than inhibiting IDO, which causes growth delay but not tumor regression as we have previously shown (*44*). However, combining an IDO inhibitor with VO-OHpic conferred additional benefit, delaying the regrowth of the tumor and prolonging the duration of response (fig. S17A). This was consistent with our in vitro model, in which PTEN maintained the function of T_{regs} that were already activated, but IDO contributed to activation of new T_{regs}. LLC lung carcinoma tumors also showed synergy between chemotherapy and inhibition of PTEN (fig. S17B).

Immune activation after chemotherapy when PTEN is inhibited

When PTEN was inhibited, the response of the host immune system to chemotherapy became fundamentally changed. Phosphorylation of Akt in T_{regs} went up (Fig. 5B), with associated loss of FoxO3a expression (Fig. 5C). T_{regs} were destabilized, as shown by reprogramming (expression of IL-2 and CD40L, Fig. 5C, lower panels). DCs acquired the activated myeloid DC phenotype ($CD11b^+CD103^+$) and many began to express IL-6, whereas PD-L1 was reduced and CD86 was markedly increased (Fig. 5D). In contrast, the T_{regs} and DCs from control mice receiving the PI3K-δ inhibitor CAL-101 showed none of these changes (Fig. 5, B to D). Functionally, both CAL-101 and VO-OHpic enhanced the antitumor effect of CTX, but VO-OHpic drove more sustained tumor regression (fig. S18). We hypothesized that the response to VO-OHpic might be related to the beneficial inflammatory effects of the destabilized (reprogrammed) T_{regs}. To test this, tumors were grown in mice with a transgenic diphtheria toxin receptor (DTR) under the control of the Foxp3 promoter, thus allowing global depletion of T_{regs} by administration of diphtheria toxin (DT, fig. S19). Ablation of T_{regs} with DT modestly enhanced the effect of CTX, but this effect was much less than the effect of VO-OHpic, and tumors showed no regression. When mice received both VO-OHpic and T_{reg} ablation, the superior efficacy of VO-OHpic was lost, and the response became equivalent to DT ablation alone. Thus, the destabilized T_{regs} appeared to be an important driver of the antitumor response.

To directly test this, we bred mice that lacked the ability to undergo T_{reg} reprogramming by ablating the IL-6 receptor on T_{regs} (IL6R^{Treg}-KO mice). We have previously shown that IL-6 is required to drive T_{reg} reprogramming (*22*, *38*), which has also been seen by others (*45*, *46*). T_{regs} from IL6R^{Treg}-KO mice were unable to reprogram in vitro (fig. S20A). In vivo, treatment with CTX + VO-OHpic lost all antitumor effect (fig. S20, B and C). Thus, T_{reg} reprogramming was functionally required for the synergy between VO-OHpic and chemotherapy, consistent with the role of PTEN in maintaining T_{reg} stability (*20*, *21*).

We next tested the contribution of effector $CD8^+$ T cells. Studies in Rag-deficient mice showed that adaptive immunity was strictly required (Fig. 5E). To follow a known population of tumor-reactive $CD8^+$ T cells during treatment, we pretransferred a cohort of Thy1.1 congenic pmel-1 T cells into normal wild-type host mice before implanting tumors (Fig. 5F). In untreated mice, pmel-1 cells in the tumor appeared unactivated (no expression of CD69, 1B11, or IFN-γ) and many expressed PD-1, suggestive of an exhausted phenotype. In contrast, when mice were treated with CTX + VO-OHpic, the pmel-1 cells in tumors down-regulated PD-1, and many now expressed CD69, 1B11, and IFN-γ. Finally, we used antibody-mediated depletion to determine whether endogenous $CD8^+$ T cells were required. Depletion of $CD8^+$ cells completely abrogated the antitumor effect of CTX + VO-OHpic (Fig. 5G), and the intratumoral T_{regs} did not lose their FoxO3a$^+$ PD-1$^+$ (suppressive) phenotype. This was consistent with our previous reports (*22*) showing that T_{reg} destabilization is an active process, driven by activated effector T cells.

Together, across multiple experiments using B16F10, EL4, LLC, and autochthonous Tg(*Grm1*)Epv tumors, we observed consistent reconfiguration of the tumor milieu into a proinflammatory phenotype after CTX + VO-OHpic (Fig. 5H). These changes closely recapitulated the spontaneous changes seen when tumors were grown in genetically defined PTEN^{Treg}-KO mice (cf. Fig. 2). Similarly, fig. S21 shows that tumors in wild-type mice treated with CTX + VO-OHpic became indistinguishable from tumors grown in PTEN^{Treg}-KO hosts, whereas, conversely, tumors grown in PTEN^{Treg}-KO mice showed no further discernible effect of CTX + VO-OHpic. Thus, although PTEN can be expressed in multiple cell types, its expression in T_{regs} appeared to be an important target of VO-OHpic in tumor-bearing hosts.

Rapid regression of autochthonous tumors

Autochthonous tumors coevolve with the host immune system. This creates profound immune tolerance, and such tumors are much more resistant to the immunologic effects of chemotherapy than transplantable tumors (*47*). To test the role of PTEN in a demanding autochthonous setting, we used Tg(*Grm1*)Epv mice (*48*), which express the oncogenic

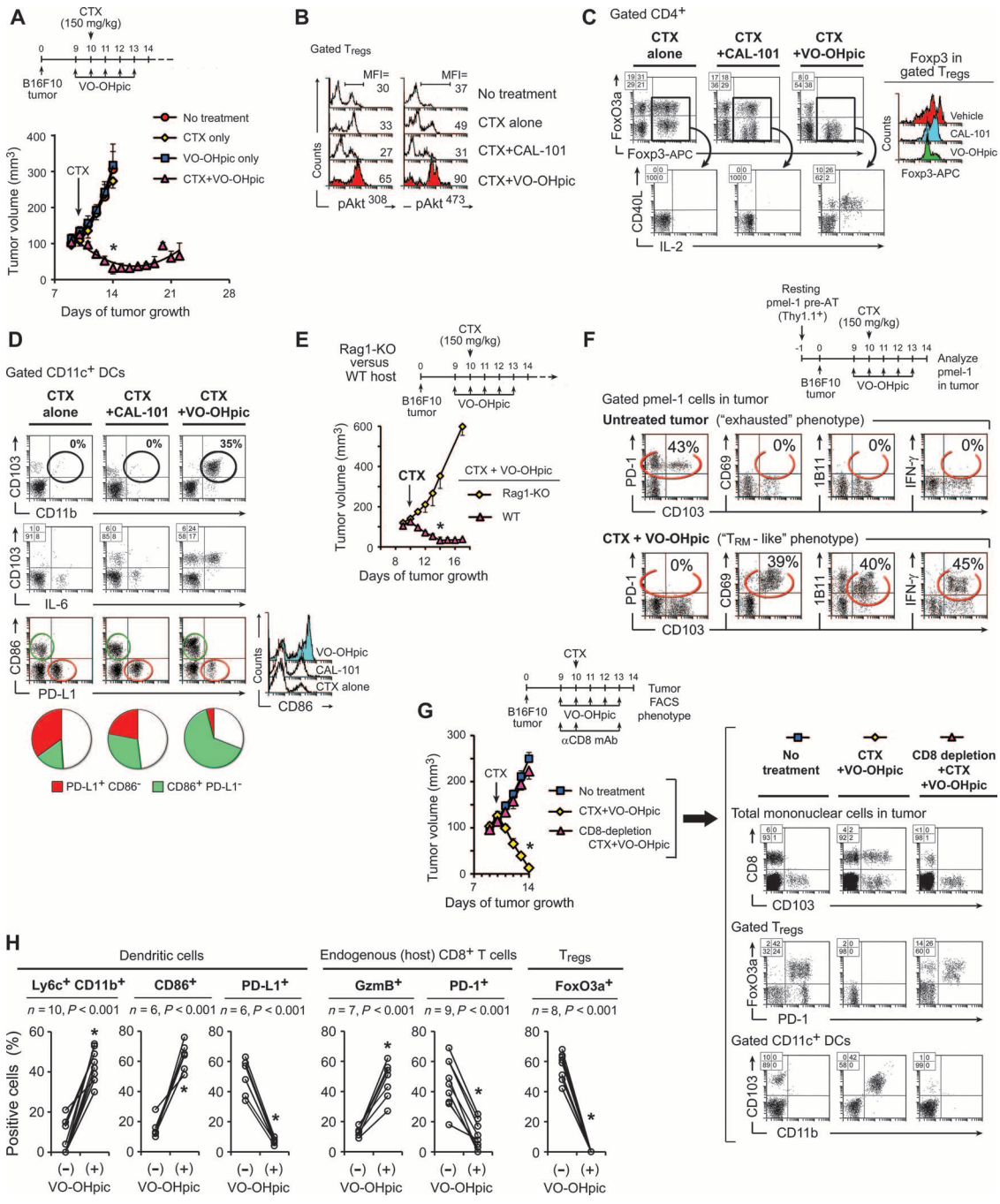

Fig. 5. Blocking PTEN allows rapid, spontaneous reconfiguration of the suppressive tumor milieu after chemotherapy. (**A**) WT B6 mice with established B16F10 tumors were treated with a single dose of CTX (150 mg kg^{-1} ip) with or without VO-OHpic (10 mg kg^{-1} day^{-1} ip). Tumor volume is shown. Pooled data from five independent experiments; $n = 10$ to 16 tumors in each group; bars show SD. *$P < 0.01$ versus all other groups by ANOVA. (**B** to **D**) Mice with B16F10 tumors were treated as in (A) with CTX plus either VO-OHpic, CAL-101, or vehicle. (B) Phosphorylation of Akt in tumor-associated T_{regs} was assessed 4 days after CTX [numbers show the mean fluorescence intensity (MFI) of the positive population]. (C) T_{reg} reprogramming in tumors after chemotherapy. Inset histograms show reduction in Foxp3 fluorescence with VO-OHpic. (D) DC activation in tumors after chemotherapy with VO-OHpic. (**E**) Rag1-KO hosts or WT B6 controls treated with CTX plus VO-OHpic. Mean of 16 tumors from two independent experiments; bars show SD (the bars in the WT group are smaller than the symbols). *$P < 0.01$ by ANOVA. (**F**) B6 mice received 2×10^6 Thy1.1-congenic resting pmel-1 cells and then were implanted with B16F10 tumors. After 9 days, mice received either CTX + VO-OHpic or no treatment, and the phenotype of pmel-1 cells in tumors was analyzed on day 14. Representative of three experiments. (**G**) The effect of CTX + VO-OHpic is abrogated by antibody-mediated depletion of $CD8^+$ cells. FACS analysis of tumor-infiltrating cells from representative tumors is shown on the right. $n = 6$ tumors per group, pooled from three independent experiments, *$P < 0.01$ by ANOVA. (**H**) Aggregate phenotyping data for immune cells infiltrating tumors treated with CTX, with or without VO-OHpic. The number of independent experiments for each marker is given, with P value by two-tailed paired t test. Lines connect the two groups in each experiment.

Grm1 receptor under the melanocyte-specific Trp2 promoter. These mice progressively develop extensive multifocal melanomas on the ears and tail. When tumors became extensive (4 to 6 months of age), mice were treated with one dose of CTX plus VO-OHpic for 6 days. After treatment, even large, multifocal confluent tumors rapidly regressed (Fig. 6A). As a measure of regression, we used ear thickness as a proxy, because all ears were extensively involved with tumor (inset graph, Fig. 6A). Control groups receiving chemotherapy alone, VO-OHpic alone, or no treatment all showed no detectable effect (shown as the pooled controls on the graph). All the effects of CTX + VO-OHpic were lost when mice received depleting monoclonal antibody (mAb) against CD8 (upper inset graph), confirming that the effect was immune-dependent. Histologically, regression was accompanied by a selective elimination of the melanotic tumor cells, leaving underlying tissue intact (Fig. 6B). FACS analysis of regressing tumors showed emergence of the characteristic $Ly6c^+CD11b^+$-activated myeloid DCs (Fig. 6C), identical to those in the transplantable tumor models mentioned earlier. Tumor-infiltrating host $CD8^+$ T cells lost their $PD\text{-}1^+$ exhausted phenotype and up-regulated granzyme B (Fig. 6D). All T_{regs} in the tumor lost detectable FoxO3a and PD-1 expression after treatment (Fig. 6E), and the T_{regs} became unstable and began to express CD40L and IL-2 (Fig. 6F). Thus, even in mice with extensive, multifocal autochthonous tumors, a single dose of chemotherapy caused rapid and widespread tumor regression when PTEN was inhibited.

DISCUSSION

Here, we identify PTEN signaling in T_{regs} as an important, centrally positioned driver of the immunosuppressive milieu in tumors. When this pathway was active, T_{regs} in tumors were highly suppressive; the antigen-presenting cell (APC) population was dominated by PD-L1–expressing DCs, with little evidence of inflammation or cross-presentation, and $CD8^+$ T cells appeared unactivated and exhausted in the tumor.

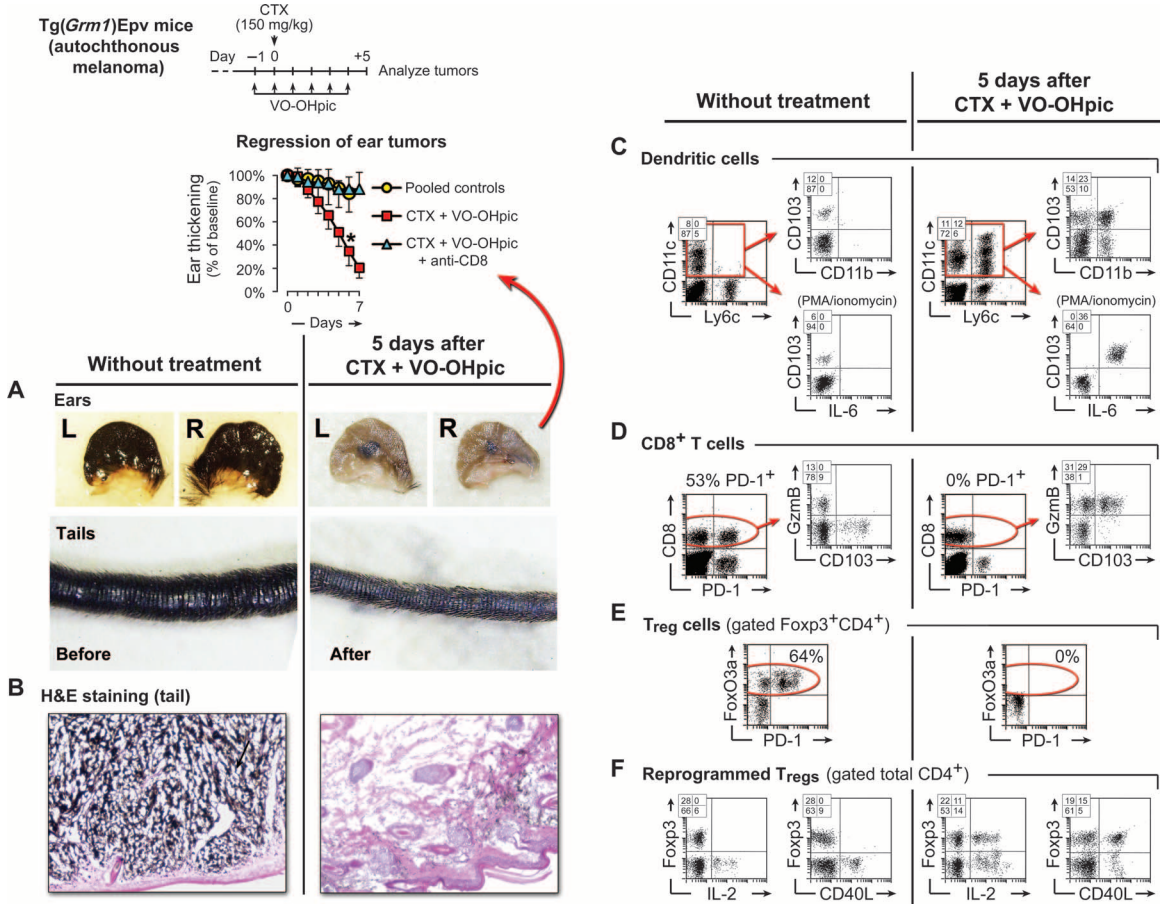

Fig. 6. Extensive autochthonous melanoma tumors regress after chemotherapy plus PTEN inhibitor. Tg(*Grm1*)Epv mice with extensive, multifocal autochthonous melanomas were treated with a single dose of CTX plus VO-OHpic as shown. Some mice also received concurrent CD8-depleting antibody as described in Materials and Methods. (**A**) Regression of tumors on the ears and tail (ears are from representative mice; tails are before and after). Inset graph: quantitation of ear thickness (proxy for tumor involvement) after treatment. n = 10 to 16 ears per group serially measured from three independent experiments; bars show SD. *P < 0.01 by ANOVA versus all other groups. The "pooled controls" group contains CTX alone and VO-OHpic alone, neither of which showed any effect. To estimate tumor regression, we subtracted the normal thickness of healthy mouse ear (0.6 ± 0.03 mm, n = 12) and then we expressed the serial tumor measurements as percent change relative to the original pretreatment baseline for that ear. (**B**) Histology on day +4 of CTX/VO-OHpic [hematoxylin and eosin (H&E) stain; tumor cells are visible as black melanotic lesions]. Representative of four experiments. (**C** to **F**) Phenotype of cells from disaggregated tumor (several pooled tumors from the same mouse). Representative of five independent experiments.

In contrast, if the PTEN pathway was ablated in T_{regs}, then the same tumors became spontaneously inflammatory and immunogenic: T_{regs} in the tumor (but not elsewhere) lost their suppressive phenotype and converted into proinflammatory helper cells (ex-T_{regs}); the major DC population was changed into a characteristic population of activated myeloid DCs expressing Ly6c, CD11b, and CD103 and producing IL-6; costimulation (CD86) went up and co-inhibition (PD-L1) went down; and $CD8^+$ T cells became activated in the tumor. Thus, the PTEN pathway in T_{regs} dominantly regulated a suite of critical downstream pathways.

Tumors rely on multiple immunosuppressive mechanisms; thus, PTEN-T_{regs} are a part of a larger network, but it was striking that a single pathway in a single cell type was so crucial for the overall immunologic milieu of the tumor. PTEN-T_{regs} were found in three different transplantable tumors and in each of the spontaneous tumors tested in an autochthonous tumor model. It is not yet known how these different tumors all converged on the same suppressive pathway, but insight may come from our finding that $PTEN^{Treg}$-KO mice were unable to suppress immune responses to apoptotic cells. Tumors are aberrant and have a high rate of constitutive cell turnover—in many respects, they resemble chronic wounds (*49*). This chronic, ongoing cell death can become massively increased after chemotherapy or immunotherapy. Thus, the ability to enforce immune suppression in response to apoptotic cells may be an important immune-evasion pathway for tumors, particularly under the stress of chemotherapy or vaccination.

PTEN had connections to the IDO pathway. IDO-activated T_{regs} became dependent on PD-1→PTEN signaling to maintain their suppression, whereas apoptotic tumor cells actively induced PTEN-T_{regs} in an IDO-dependent fashion. However, the tumor-resistant phenotype of $PTEN^{Treg}$-KO mice was much more robust than that of IDO1-KO mice, and blocking PTEN had a more acute antitumor effect than blocking IDO alone. PTEN is downstream of other important T_{reg}-activating signals as well, such as neuropilin-1 (*29*). Thus, PTEN appears to be an important nexus for multiple upstream signals in T_{reg} biology. This makes it an attractive target for therapy.

Pharmacologic inhibition of PTEN was synergistic with chemotherapy. In the case of the melanoma models [B16F10 and Tg(*Grm1*) Epv], this synergy was dramatic. Different tumor types displayed different degrees of regression after CTX + VO-OHpic, and some tumors may recruit more myeloid-derived suppressor cells or other mechanisms that are not as dependent on PTEN. Part of the susceptibility of various tumors may be dictated by the strength of the spontaneous, preexisting $CD8^+$ T cell response against the tumor. Using depletion studies, we found that endogenous host $CD8^+$ T cells were strictly required for the antitumor effect of chemotherapy + PTEN inhibitor. In addition to being cytotoxic effector cells, these $CD8^+$ cells appeared to play an important role as drivers of inflammation. Without the endogenous $CD8^+$ cells, intratumoral T_{regs} never lost their suppressive phenotype, and there was no downstream activation of inflammatory myeloid DCs. Thus, although blocking PTEN rendered the T_{regs} unstable in the face of inflammation, the $CD8^+$ T cells were required to actually trigger that inflammation itself and thus drive reprogramming.

This role for inflammation and T cells differs from the older concept that the immune system might contribute some of the intrinsic efficacy of standard chemotherapy (that is, chemotherapy used by itself) (*50*). Our model does not speak to this, because we deliberately chose a chemotherapy regimen that had no efficacy by itself against the tumor. It was only when the PTEN inhibitor was added, and new immunologic mechanisms were now unleashed, that the combined chemoimmunotherapy regimen showed efficacy. It was this new, synergistic effect of the combination that was strictly immune-dependent.

PTEN-T_{regs} were indispensable for regulating the immune response to apoptotic cells. In mice without tumors, simply injecting apoptotic tumor cells caused rapid local activation of PTEN-T_{regs}, and T cell responses to cell-associated antigens were suppressed. However, if PTEN was blocked or ablated, then the same apoptotic tumor cells were now treated as proinflammatory and caused activation of DCs and cross-presentation of antigen to T cells. Thus, whether the host treated apoptotic cells as immunogenic or tolerogenic was not intrinsic to the dying cells themselves, but rather was a choice enforced by the activated PTEN-T_{regs}. Consistent with this, when $PTEN^{Treg}$-KO mice were challenged with repetitive injections of apoptotic thymocytes, they rapidly developed multiple lupus-like autoantibodies. This phenotype is very similar to IDO1-deficient mice, challenged with the same regimen of apoptotic cells (*23*), which is consistent with our finding that apoptotic cells induced PTEN-T_{regs} via IDO. Thus, we hypothesize that one normal role of the PTEN-T_{reg} pathway is to maintain self-tolerance to apoptotic cells, and this natural tolerogenic pathway is pathologically co-opted by tumors.

Other strains of mice lacking PTEN in T_{regs} spontaneously develop lupus autoantibodies as they age (*20*, *21*). Our mice, using a different Cre system and different PTEN-floxed mice, had a somewhat milder phenotype and did not develop autoantibodies until late in life. However, both strains developed the same lupus-like autoimmunity, with its characteristic autoantibody response against antigens derived from apoptotic cells. The fact that our strain had late onset of disease was crucial, because it allowed us to demonstrate the markedly and fundamentally altered underlying response to tumors, even in healthy, asymptomatic young mice.

The role of PTEN in self-tolerance introduces the possibility of autoimmune side effects when PTEN inhibitors are used therapeutically. Autoimmunity is always a potential "on-target" toxicity for strategies that aim to break tolerance to tumor cells (*51*). However, the PTEN pathway has several attributes that make it attractive for clinical therapy. First, the required duration of inhibitor treatment is brief, being focused just on the specific period when tumor cells are undergoing cell death after chemotherapy or vaccination. Second, the tumor appears to be heavily dependent on the PTEN-T_{reg} pathway for immunosuppression, much more so than normal tissues. This was shown by the spontaneous inflammation seen within the tumor in young, healthy $PTEN^{Treg}$-KO mice but not seen anywhere else outside the tumor. Third, tumors are mutated and hence potentially more immunogenic than normal tissues (*52*). This may contribute to the "driver" CD8 response needed to initiate inflammation within the tumor.

Together, these factors may allow brief, focused dosing with the PTEN inhibitor to achieve selective effects on the tumor while minimizing autoimmune toxicity. The use of intermittent dosing also mitigates the hypothetical concern that PTEN inhibitors might be oncogenic. PTEN is a tumor-suppressor gene, but it is not a transforming oncogene; thus, to have an oncogenic effect, it must be inhibited for a prolonged period and also combined with additional driver oncogenes. Hence, transient intermittent interruption and restoration of PTEN should not be an oncogenic regimen and may actually cause senescence in tumor cells (*53*). Together, our findings identify the PTEN pathway in T_{regs} as an important driver of the

immunosuppressive tumor microenvironment and a potentially attractive target for therapy.

MATERIALS AND METHODS

Reagents

Indoximod (1-methyl-D-tryptophan) and NLG919 were supplied as clinical-grade material by NewLink Genetics Inc. For in vitro studies, indoximod was dissolved in alkaline pH as previously described (*34*) and diluted in phosphate-buffered saline (PBS) at a final pH of 7.4. Rapamycin (Sigma #R8781) was used at 85 nM. PP242 (Seleckchem #S2218) was used at 100 nM. Human $gp100_{25–33}$ (KVPRNQDWL) and SIINFEKL peptides were synthesized by Southern Biotechnology from the published sequence (*54*, *55*). VO-OHpic (BioVision #1801-5) was used at 1 μM in vitro unless otherwise specified (*37*) and at 10 mg kg^{-1} day^{-1} in vivo, administered in 10% dimethyl sulfoxide (DMSO). CAL-101 (Seleckchem #S2226) was used at 200 nM in vitro and at 30 mg kg^{-1} day^{-1} in vivo, administered in 10% DMSO.

T_{reg}/DC cocultures

Initial activation cocultures. Our T_{reg} coculture system has been previously described (*22*, *24*). Cocultures were performed in V-bottom wells (Nunc 249952 V96) to ensure cell-cell contact. Rapid isolation of T_{regs} was important; hence, LNs and spleen were mechanically disaggregated by passing once through a 40-μm mesh and then briefly stained on ice and FACS-sorted into ice-cold medium using low-shear fluidics and a large nozzle. IDO^+ DCs (5×10^3 per well) were enriched from TDLNs of B16F10 tumors (days 7 to 11) by sorting for $CD11c^+$ cells, which typically contained 30 to 40% IDO^+ DCs (*24*); because the effects of IDO were dominant, further fractionation was not necessary. Resting T_{regs} (2×10^4 per well) were sorted as $CD4^+GFP^+$ cells from spleens of *Foxp3*^{GFP}, *Foxp3*$^{DTR\text{-}GFP}$, or *Foxp3*$^{GFP\text{-}Cre}$ mice; all three strains gave equivalent results. $CD8^+$ effector cells (5×10^4) were FACS-sorted from spleens of OT-I or pmel-1 mice and added to cocultures with 100 nM cognate peptide (either SIINFEKL or hgp100). All cultures received a feeder layer of 1×10^5 T cell–depleted B6 spleen cells ($CD4^{NEG}CD8^{NEG}$) to maintain T_{reg} viability, as previously described (*24*). Cultures received either indoximod (200 μM) or NLG919 (1 μM) to inhibit IDO. For αCD3-induced activation, cocultures received αCD3 mAb (0.1 μg/ml; clone 145-2C11, azide-free); in addition, these cultures also always received an IDO inhibitor to ensure that IDO was not active or inducible during coculture.

T_{reg} re-sorting and readout assays. After 2 to 3 days (the time was not critical), activation cocultures were harvested, cells were stained for CD4, and the activated T_{regs} were re-sorted as $CD4^+GFP^+$ cells. For readout assays, sorted T_{regs} were added to V-bottom wells containing 5×10^4 FACS-sorted $CD8^+$ effector cells (OT-I or pmel-1, as used in the original activation cultures) plus 5×10^3 $CD11c^+$ DCs sorted from normal LNs of mice without tumors. Some wells received blocking antibodies against the PD-1 pathway, as a cocktail (each 50 μg/ml) of anti–PD-L2, clone TY25 (*56*); anti–PD-1, clone J43 (*57*); and anti–PD-L1, clone MIH7 (*58*) (a gift of M. Azuma). After 3 days, cocultures were analyzed by flow cytometry or were pulsed with [^{3}H]thymidine to measure proliferation.

Ex vivo T_{reg} assays from vaccine-draining LNs. To measure spontaneous T_{reg} activity in vaccine-draining LNs (VDLNs), we implanted B16F10 tumors in Foxp3-GFP reporter mice. On day 11, mice received hgp100 vaccine in CpG/IFA (incomplete Freund's adjuvant) in the contralateral footpad, with intravenous pmel-1 adoptive transfer. Three days later, the VDLNs were harvested and $CD4^+GFP^+$ T_{regs} were sorted and added to readout assays as described in the preceding section.

Antibodies and FACS staining

LNs were prepared by rapidly passing through a 40-μm mesh and then stained using short incubation times (10 min on ice), as previously described (*22*). Tumors were disaggregated by treating for 1 hour with collagenase (1 mg/ml; C5138, Sigma), deoxyribonuclease (0.1 mg/ml; D5025, Sigma), and hyaluronidase (0.1 mg/ml; H3884, Sigma) in RPMI 1640 medium.

Conjugated mAbs against the following were from BD Biosciences: CD4 (clone RM4-5), CD8α (clone 53-6.7), CD80 (clone 16.10A1), CD86 (clone GL1), CD11c (clone HL3), Ly6c (clone AL-21), PTEN (A2B1), CD25 (clone PC61), IFN-γ (clone XMG1.2), CD24 (clone M1/69), and B220 (clone RA3-6B2). Conjugated antibodies against the following were obtained from eBioscience: Foxp3 (clone FJK-16s), granzyme B (clone NGZB), PD1 (clone J43), PD-L1 (clone MIH5), PD-L2 (clone 122), CD103 (Ber-ACT8) and Ly6c (clone HK1.4), CD278 (ICOS, clone 7E.17G9), CD69 (clone H1.2F3), IL-2 (clone JES6-5H4), IL-17A (clone 17B7), CD40L (clone MR1), IL-6 (clone MP5-20F3), CD11b (clone M1/70), and CD126 (clone D7715A7). Clone 1B11 (glycosylated CD43) was from BioLegend.

Intracellular antigens were detected using a fixation-permeabilization reagent and a matching perm-wash buffer from eBioscience (catalog #00-5521), with blocking using 5% normal donkey serum, and then acquired immediately after staining. IL-2, IFN-γ, and IL-6 were measured after 4 hours of activation with PMA/ionomycin in the presence of brefeldin A as previously described (*22*). Unconjugated anti-FoxO3a (4 μg/ml; rabbit mAb, clone 75D8, Cell Signaling Technology) was used in the perm-wash buffer and was detected with donkey anti-rabbit PE (Jackson ImmunoResearch #711-116-152) at 1:100 dilution. All washes were performed in the perm-wash buffer in the cold. Goat anti-Eos (sc-132308) (2 μg/ml) from Santa Cruz Biotechnology was used, followed by cross-adsorbed secondary donkey anti-goat APC (705-136-147) from Jackson ImmunoResearch as previously described (*22*).

For phospho-specific staining, antibodies were from Cell Signaling Technology, either Alexa Fluor 647–conjugated pAkt-Thr^{308} (catalog #3375), pAkt-Ser^{473} (catalog #4075), or anti-pS6 (catalog #4851). Cells were washed in PBS, fixed with 2% paraformaldehyde for 10 min at 37°C, prechilled for 1 min, and then permeabilized by slow addition of ice-cold methanol to a final concentration of 90%. Cells were then incubated on ice for 30 min, washed with 1% fetal calf serum/PBS, blocked with the same solution for 10 min at room temperature and then for 1 hour at room temperature, and washed. Cells were acquired immediately after staining.

Mouse strains

All animal studies were approved by the Institutional Animal Care and Use Committee of Georgia Health Sciences University. FoxO3-deficient mice (FoxO3Kca strain) have been previously described (*28*) and were the gift of S. Hedrick and the Ludwig Institute for Cancer Research. The following were obtained from the Jackson Laboratory and bred in our colony: OT-I mice [$CD8^+$, recognizing the SIINFEKL peptide of OVA on $H2K^b$ (*55*)] and pmel-1 mice [B6.Cg-*Thy1*^{a}/CyTg(TcraTcrb)8Rest/J, recognizing a peptide from human gp100 (*54*)].

IDO-deficient mice (B6 background) have been previously described (*59*, *60*). PD-1–deficient mice have been previously described (*26*).

T_{regs} were identified using GFP reporter mice. To ensure that results were not influenced by a particular reporter strain, we confirmed them using multiple reporter systems. *Foxp3*^{GFP} mice (*61*, *62*), bearing a Foxp3-GFP fusion protein in the coding region of the Foxp3 locus, were the gift of A. Rudensky. *Foxp3*^{DTR} mice, with a DTR-GFP fusion construct knocked in to the 3′ untranslated region of the Foxp3 gene (but with a normal Foxp3 coding sequence), were the gift of A. Rudensky (*63*). Mice with a BAC-transgenic GFP-Cre fusion protein under the Foxp3 promoter (*Foxp3*$^{GFP\text{-}Cre}$) (*36*, *64*) were obtained from the Jackson Laboratory [NOD/ShiLt-Tg(Foxp3-EGFP/cre)1Jbs/J] and backcrossed in our colony onto the B6 background. These were used for intercrosses with floxed alleles to create T_{reg}-specific deletions, as follows.

PTEN^{Treg}*-KO mice*: *Foxp3*$^{GFP\text{-}Cre}$ mice, as described above, were crossed with mice bearing *loxP* sites flanking exon 5 of the PTEN gene (B6.129S4-Pten^{tm1Hwu}/J, Jackson Laboratory) (*35*). The resulting strain was maintained as hemizygous for GFP-Cre and homozygous for *Pten*$^{loxP/loxP}$.

FoxO3^{Treg}*-KO mice*: *Foxp3*$^{GFP\text{-}Cre}$ mice were crossed with mice bearing *loxP* sites flanking exon 2 of the *Foxo3* gene (a gift of R. DePinho and the Dana-Farber Cancer Institute) (*65*). The resulting strain was maintained as hemizygous for GFP-Cre and homozygous for *Foxo3*$^{loxp/loxp}$. These mice were used as controls to validate the specificity of FoxO3a intracellular staining.

IL6Ra^{Treg}*-KO mice*: *Foxp3*$^{GFP\text{-}Cre}$ mice were crossed with mice bearing *loxP* sites flanking exons 4 to 6 of the IL-6 receptor α-chain (*Il6ra*) gene (B6;SJL-Il6ra$^{tm1.1Drew}$/J, Jackson Laboratory) (*66*). The resulting strain was maintained as hemizygous for GFP-Cre and homozygous for *IL6ra*$^{loxp/loxp}$.

Tumor studies

The Tg(*Grm1*)Epv mouse strain (*48*) was the gift of S. Chen (Rutgers University). The B16F10, EL4, E.G7, and LLC cell lines were from the American Type Culture Collection. B16-OVA (B16F10 transfected with full-length chicken OVA) clone MO4 (*67*) was the gift of A. Houghton (Memorial Sloan Kettering). Tumor implantation was performed as previously described (*24*), using 1×10^5 cells for B16F10 and 1×10^6 cells for other cell lines (large inocula were used to ensure rapid tumor engraftment and immune suppression). Tumor volume was calculated from orthogonal diameters using the formula $V = L \times W^2 \times \pi/6$. Indoximod (2 mg/ml) was administered in drinking water as previously described (*24*), and NLG919 (6 mg/ml) was similarly administered. VO-OHpic was given at 10 mg kg^{-1} day^{-1} ip in 10% DMSO. CAL-101 was given at 30 mg kg^{-1} day^{-1} ip in 10% DMSO. For in vivo CD8 depletion studies, mice received anti-CD8 antibody clone YTS 169.4 (BioXcell) given at 200 μg ip 1 day before CTX and then at 100 μg ip every other day throughout the experiment. Indoximod (2 mg/ml; D-1MT) was administered in drinking water as previously described (*24*). Mice received approved euthanasia when tumors reached a size of 300 mm^2 (product of orthogonal diameters); death was not used as a planned end point in any study.

Vaccines and T cell adoptive transfers

CpG-1826 (phosphorothioate oligo 5′-TCCATGACGTTCCTGAGCTT-3′) was synthesized from the published sequence (*68*) by TriLink Biotechnologies. Whole OVA protein was from Sigma (#A-5503). Human gp100$_{25–33}$ was synthesized from the published sequence (*54*). Vaccines were prepared with 100 μg of OVA protein or 25 μg of peptide, with 50 μg of CpG-1826 in IFA (Sigma F-5506) and administered in the hindlimb footpad. Popliteal LNs were harvested 4 days later. For all adoptive transfers, OT-I or pmel-1 spleen cells were enriched by negative selection using magnetic beads (mouse CD8 isolation kit II, #130-095-236, Miltenyi Biotec). Staining for bead isolation was performed on ice, with short incubation times. Mice received 2×10^6 enriched CD8$^+$ cells via the tail vein.

Statistics

Multiple treatment groups were compared by ANOVA with Tukey's honestly significant difference correction. Independent replicates for each experiment in the manuscript are indicated in the figure legends. Error bars always show SD.

SUPPLEMENTARY MATERIALS

Supplementary material for this article is available at http://advances.sciencemag.org/cgi/content/full/1/10/e1500845/DC1

Methods

Fig. S1. Extended phenotyping of T_{reg} population in LNs of normal mice, in TDLNs of mice with B16F10 tumors, and in the disaggregated tumors themselves.

Fig. S2. Role of IDO, PD-1, and mTOR pathways during T_{reg} activation in vitro.

Fig. S3. In vivo phosphorylation status of S6 and Akt^{473} in T_{regs} from TDLNs of tumor-bearing mice, after vaccination in the presence or absence of IDO inhibitor drug (2 mg/ml in drinking water, or vehicle control, as indicated).

Fig. S4. Confirmation of specificity of the FoxO3a staining antibody (rabbit monoclonal, clone 75D8, Cell Signaling Technology).

Fig. S5. Foxo3a in activated T_{regs} in vitro.

Fig. S6. Activation step cocultures using IDO$^+$ TDLN DCs were supplemented with excess tryptophan at the concentrations shown.

Fig. S7. IDO was important in controlling Akt phosphorylation, but it was unclear how IDO, which was expressed in the DCs, influenced the mTOR→Akt^{473} pathway expressed in T_{regs}.

Fig. S8. Role of PD-1 in maintaining IDO-induced suppressor activity.

Fig. S9. Validation of PTEN^{Treg}-KO mice.

Fig. S10. Growth of EL4-OVA (E.G7) and LLC tumors in PTEN^{Treg}-KO hosts.

Fig. S11. Spontaneous reprogramming of T_{regs} in tumors of PTEN^{Treg}-KO mice.

Fig. S12. Inflammatory intratumoral milieu in E.G7 tumors grown in PTEN^{Treg}-KO hosts.

Fig. S13. Artifactual preactivation by CD8 bead isolation obscures immunosuppression by tumors.

Fig. S14. T_{regs} were activated using IDO$^+$ TDLN DCs (**left**) or with αCD3 mitogen and IDO blocked (**right**).

Fig. S15. Effect of PTEN blockade or genetic deletion on response to vaccination.

Fig. S16. Absence of autoantibodies in mice receiving VO-OHpic.

Fig. S17. Combination of VO-OHpic with indoximod.

Fig. S18. Comparison of VO-OHpic versus CAL-101 when given in combination with CTX.

Fig. S19. B16F10 tumors were grown in mice bearing an insertion of a fusion protein of GFP with the human DTR into the Foxp3 locus (*63*).

Fig. S20. Requirement for IL-6 receptor expression on T_{regs} for T_{reg} destabilization and anti-tumor response.

Fig. S21. PTEN^{Treg}-KO mice lose any further effect of the VO-OHpic PTEN inhibitor.

REFERENCES AND NOTES

1. F. Duan, J. Duitama, S. Al Seesi, C. M. Ayres, S. A. Corcelli, A. P. Pawashe, T. Blanchard, D. McMahon, J. Sidney, A. Sette, B. M. Baker, I. I. Mandoiu, P. K. Srivastava, Genomic and bioinformatic profiling of mutational neoepitopes reveals new rules to predict anticancer immunogenicity. *J. Exp. Med.* **211**, 2231–2248 (2014).
2. P. G. Coulie, B. J. Van den Eynde, P. van der Bruggen, T. Boon, Tumour antigens recognized by T lymphocytes: At the core of cancer immunotherapy. *Nat. Rev. Cancer* **14**, 135–146 (2014).
3. M. M. Gubin, X. Zhang, H. Schuster, E. Caron, J. P. Ward, T. Noguchi, Y. Ivanova, J. Hundal, C. D. Arthur, W.-J. Krebber, G. E. Mulder, M. Toebes, M. D. Vesely, S. S. K. Lam, A. J. Korman, J. P. Allison, G. J. Freeman, A. H. Sharpe, E. L. Pearce, T. N. Schumacher, R. Aebersold,

H.-G. Rammensee, C. J. M. Melief, E. R. Mardis, W. E. Gillanders, M. N. Artyomov, R. D. Schreiber, Checkpoint blockade cancer immunotherapy targets tumour-specific mutant antigens. *Nature* **515**, 577–581 (2014).
4. A. Snyder, V. Makarov, T. Merghoub, J. Yuan, J. M. Zaretsky, A. Desrichard, L. A. Walsh, M. A. Postow, P. Wong, T. S. Ho, T. J. Hollmann, C. Bruggeman, K. Kannan, Y. Li, C. Elipenahli, C. Liu, C. T. Harbison, L. Wang, A. Ribas, J. D. Wolchok, T. A. Chan, Genetic basis for clinical response to CTLA-4 blockade in melanoma. *N. Engl. J. Med.* **371**, 2189–2199 (2014).
5. E. Cha, M. Klinger, Y. Hou, C. Cummings, A. Ribas, M. Faham, L. Fong, Improved survival with T cell clonotype stability after anti–CTLA-4 treatment in cancer patients. *Sci. Transl. Med.* **6**, 238ra70 (2014).
6. A. Gros, P. F. Robbins, X. Yao, Y. F. Li, S. Turcotte, E. Tran, J. R. Wunderlich, A. Mixon, S. Farid, M. E. Dudley, K.-. Hanada, J. R. Almeida, S. Darko, D. C. Douek, J. C. Yang, S. A. Rosenberg, PD-1 identifies the patient-specific $CD8^+$ tumor-reactive repertoire infiltrating human tumors. *J. Clin. Invest.* **124**, 2246–2259 (2014).
7. P. C. Tumeh, C. L. Harview, J. H. Yearley, I. P. Shintaku, E. J. M. Taylor, L. Robert, B. Chmielowski, M. Spasic, G. Henry, V. Ciobanu, A. N. West, M. Carmona, C. Kivork, E. Seja, G. Cherry, A. J. Gutierrez, T. R. Grogan, C. Mateus, G. Tomasic, J. A. Glaspy, R. O. Emerson, H. Robins, R. H. Pierce, D. A. Elashoff, C. Robert, A. Ribas, PD-1 blockade induces responses by inhibiting adaptive immune resistance. *Nature* **515**, 568–571 (2014).
8. C. Reissfelder, S. Stamova, C. Gossmann, M. Braun, A. Bonertz, U. Walliczek, M. Grimm, N. N. Rahbari, M. Koch, M. Saadati, A. Benner, M. W. Büchler, D. Jäger, N. Halama, K. Khazaie, J. Weitz, P. Beckhove, Tumor-specific cytotoxic T lymphocyte activity determines colorectal cancer patient prognosis. *J. Clin. Invest.* **125**, 739–751 (2015).
9. D. S. Chen, I. Mellman, Oncology meets immunology: The cancer-immunity cycle. *Immunity* **39**, 1–10 (2013).
10. H. Nishikawa, S. Sakaguchi, Regulatory T cells in cancer immunotherapy. *Curr. Opin. Immunol.* **27**, 1–7 (2014).
11. P. D. Bos, G. Plitas, D. Rudra, S. Y. Lee, A. Y. Rudensky, Transient regulatory T cell ablation deters oncogene-driven breast cancer and enhances radiotherapy. *J. Exp. Med.* **210**, 2435–2466 (2013).
12. P. Yu, Y. Lee, W. Liu, T. Krausz, A. Chong, H. Schreiber, Y.-X. Fu, Intratumor depletion of $CD4^+$ cells unmasks tumor immunogenicity leading to the rejection of late-stage tumors. *J. Exp. Med.* **201**, 779–791 (2005).
13. M. W. Teng, S. F. Ngiow, B. von Scheidt, N. McLaughlin, T. Sparwasser, M. J. Smyth, Conditional regulatory T-cell depletion releases adaptive immunity preventing carcinogenesis and suppressing established tumor growth. *Cancer Res.* **70**, 7800–7809 (2010).
14. A. M. Thornton, C. A. Piccirillo, E. M. Shevach, Activation requirements for the induction of $CD4^+CD25^+$ T cell suppressor function. *Eur. J. Immunol.* **34**, 366–376 (2004).
15. A. G. Levine, A. Arvey, W. Jin, A. Y. Rudensky, Continuous requirement for the TCR in regulatory T cell function. *Nat. Immunol.* **15**, 1070–1078 (2014).
16. M. D. Rosenblum, I. K. Gratz, J. S. Paw, K. Lee, A. Marshak-Rothstein, A. K. Abbas, Response to self antigen imprints regulatory memory in tissues. *Nature* **480**, 538–542 (2011).
17. S. Malchow, D. S. Leventhal, S. Nishi, B. I. Fischer, L. Shen, G. P. Paner, A. S. Amit, C. Kang, J. E. Geddes, J. P. Allison, N. D. Socci, P. A. Savage, Aire-dependent thymic development of tumor-associated regulatory T cells. *Science* **339**, 1219–1224 (2013).
18. A. Chaudhry, A. Y. Rudensky, Control of inflammation by integration of environmental cues by regulatory T cells. *J. Clin. Invest.* **123**, 939–944 (2013).
19. A. Liston, D. H. D. Gray, Homeostatic control of regulatory T cell diversity. *Nat. Rev. Immunol.* **14**, 154–165 (2014).
20. A. Huynh, M. DuPage, B. Priyadharshini, P. T. Sage, J. Quiros, C. M. Borges, N. Townamchai, V. A. Gerriets, J. C. Rathmell, A. H. Sharpe, J. A. Bluestone, L. A. Turka, Control of PI(3) kinase in T_{reg} cells maintains homeostasis and lineage stability. *Nat. Immunol.* **16**, 188–196 (2015).
21. S. Shrestha, K. Yang, C. Guy, P. Vogel, G. Neale, H. Chi, T_{reg} cells require the phosphatase PTEN to restrain T_H1 and T_{FH} cell responses. *Nat. Immunol.* **16**, 178–187 (2015).
22. M. D. Sharma, L. Huang, J.-H. Choi, E.-J. Lee, J. M. Wilson, H. Lemos, F. Pan, B. R. Blazar, D. M. Pardoll, A. L. Mellor, H. Shi, D. H. Munn, An inherently bifunctional subset of $Foxp3^+$ T helper cells is controlled by the transcription factor Eos. *Immunity* **38**, 998–1012 (2013).
23. B. Ravishankar, H. Liu, R. Shinde, P. Chandler, B. Baban, M. Tanaka, D. H. Munn, A. L. Mellor, M. C. I. Karlsson, T. L. McGaha, Tolerance to apoptotic cells is regulated by indoleamine 2,3-dioxygenase. *Proc. Natl. Acad. Sci. U.S.A.* **109**, 3909–3914 (2012).
24. M. D. Sharma, B. Baban, P. Chandler, D.-Y. Hou, N. Singh, H. Yagita, M. Azuma, B. R. Blazar, A. L. Mellor, D. H. Munn, Plasmacytoid dendritic cells from mouse tumor-draining lymph nodes directly activate mature Tregs via indoleamine 2,3-dioxygenase. *J. Clin. Invest.* **117**, 2570–2582 (2007).
25. N. K. Crellin, R. V. Garcia, M. K. Levings, Altered activation of AKT is required for the suppressive function of human $CD4^+CD25^+$ T regulatory cells. *Blood* **109**, 2014–2022 (2007).
26. L. M. Francisco, V. H. Salinas, K. E. Brown, V. K. Vanguri, G. J. Freeman, V. K. Kuchroo, A. H. Sharpe, PD-L1 regulates the development, maintenance, and function of induced regulatory T cells. *J. Exp. Med.* **206**, 3015–3029 (2009).
27. N. Patsoukis, J. Brown, V. Petkova, F. Liu, L. Li, V. A. Boussiotis, Selective effects of PD-1 on Akt and Ras pathways regulate molecular components of the cell cycle and inhibit T cell proliferation. *Sci. Signal.* **5**, ra46 (2012).
28. Y. M. Kerdiles, E. L. Stone, D. L. Beisner, M. A. McGargill, I. L. Ch'en, C. Stockmann, C. D. Katayama, S. M. Hedrick, Foxo transcription factors control regulatory T cell development and function. *Immunity* **33**, 890–904 (2010).
29. G. M. Delgoffe, S.-R. Woo, M. E. Turnis, D. M. Gravano, C. Guy, A. E. Overacre, M. L. Bettini, P. Vogel, D. Finkelstein, J. Bonnevier, C. J. Workman, D. A. A. Vignali, Stability and function of regulatory T cells is maintained by a neuropilin-1–semaphorin-4a axis. *Nature* **501**, 252–256 (2013).
30. Y. Park, H.-S. Jin, J. Lopez, C. Elly, G. Kim, M. Murai, M. Kronenberg, Y.-C. Liu, TSC1 regulates the balance between effector and regulatory T cells. *J. Clin. Invest.* **123**, 5165–5178 (2013).
31. E. Jacinto, V. Facchinetti, D. Liu, N. Soto, S. Wei, S. Y. Jung, Q. Huang, J. Qin, B. Su, SIN1/MIP1 maintains rictor-mTOR complex integrity and regulates Akt phosphorylation and substrate specificity. *Cell* **127**, 125–137 (2006).
32. A. Brunet, A. Bonni, M. J. Zigmond, M. Z. Lin, P. Juo, L. S. Hu, M. J. Anderson, K. C. Arden, J. Blenis, M. E. Greenberg, Akt promotes cell survival by phosphorylating and inhibiting a Forkhead transcription factor. *Cell* **96**, 857–868 (1999).
33. D. R. Plas, C. B. Thompson, Akt activation promotes degradation of tuberin and FOXO3a via the proteasome. *J. Biol. Chem.* **278**, 12361–12366 (2003).
34. D. H. Munn, M. D. Sharma, B. Baban, H. P. Harding, Y. Zhang, D. Ron, A. L. Mellor, GCN2 kinase in T cells mediates proliferative arrest and anergy induction in response to indoleamine 2,3-dioxygenase. *Immunity* **22**, 633–642 (2005).
35. R. Lesche, M. Groszer, J. Gao, Y. Wang, A. Messing, H. Sun, X. Liu, H. Wu, *Cre/loxP*-mediated inactivation of the murine *Pten* tumor suppressor gene. *Genesis* **32**, 148–149 (2002).
36. X. Zhou, L. T. Jeker, B. T. Fife, S. Zhu, M. S. Anderson, M. T. McManus, J. A. Bluestone, Selective miRNA disruption in T reg cells leads to uncontrolled autoimmunity. *J. Exp. Med.* **205**, 1983–1991 (2008).
37. L. H. Mak, R. Vilar, R. Woscholski, Characterisation of the PTEN inhibitor VO-OHpic. *J. Chem. Biol.* **3**, 157–163 (2010).
38. M. D. Sharma, D.-Y. Hou, B. Baban, P. A. Koni, Y. He, P. R. Chandler, B. R. Blazar, A. L. Mellor, D. H. Munn, Reprogrammed $Foxp3^+$ regulatory T cells provide essential help to support cross-presentation and $CD8^+$ T cell priming in naive mice. *Immunity* **33**, 942–954 (2010).
39. L. Zitvogel, G. Kroemer, $CD103^+$ dendritic cells producing interleukin-12 in anticancer immunosurveillance. *Cancer Cell* **26**, 591–593 (2014).
40. E. Etemire, M. Krull, M. Hasenberg, P. Reichardt, M. Gunzer, Transiently reduced PI3K/Akt activity drives the development of regulatory function in antigen-stimulated Naïve T-cells. *PLOS One* **8**, e68378 (2013).
41. K. Ali, D. R. Soond, R. Piñeiro, T. Hagemann, W. Pearce, E. L. Lim, H. Bouabe, C. L. Scudamore, T. Hancox, H. Maecker, L. Friedman, M. Turner, K. Okkenhaug, B. Vanhaesebroeck, Inactivation of PI(3)K p110δ breaks regulatory T-cell-mediated immune tolerance to cancer. *Nature* **510**, 407–411 (2014).
42. M. D. Sharma, D.-Y. Hou, Y. Liu, P. A. Koni, R. Metz, P. Chandler, A. L. Mellor, Y. He, D. H. Munn, Indoleamine 2,3-dioxygenase controls conversion of $Foxp3^+$ Tregs to TH17-like cells in tumor-draining lymph nodes. *Blood* **113**, 6102–6111 (2009).
43. S. P. Crampton, P. A. Morawski, S. Bolland, Linking susceptibility genes and pathogenesis mechanisms using mouse models of systemic lupus erythematosus. *Dis. Model. Mech.* **7**, 1033–1046 (2014).
44. D.-Y. Hou, A. J. Muller, M. D. Sharma, J. B. DuHadaway, T. Banerjee, M. Johnson, A. L. Mellor, G. C. Prendergast, D. H. Munn, Inhibition of indoleamine 2,3-dioxygenase in dendritic cells by stereoisomers of 1-methyl-tryptophan correlates with anti-tumor responses. *Cancer Res.* **67**, 792–801 (2007).
45. X. O. Yang, R. Nurieva, G. J. Martinez, H. S. Kang, Y. Chung, B. P. Pappu, B. Shah, S. H. Chang, K. S. Schluns, S. S. Watowich, X.-H. Feng, A. M. Jetten, C. Dong, Molecular antagonism and plasticity of regulatory and inflammatory T cell programs. *Immunity* **29**, 44–56 (2008).
46. N. Komatsu, K. Okamoto, S. Sawa, T. Nakashima, M. Oh-hora, T. Kodama, S. Tanaka, J. A. Bluestone, H. Takayanagi, Pathogenic conversion of $Foxp3^+$ T cells into T_H17 cells in autoimmune arthritis. *Nat. Med.* **20**, 62–68 (2014).
47. M. Ciampricotti, C.-S. Hau, C. W. Doornebal, J. Jonkers, K. E. de Visser, Chemotherapy response of spontaneous mammary tumors is independent of the adaptive immune system. *Nat. Med.* **18**, 344–346 (2012).
48. P. M. Pollock, K. Cohen-Solal, R. Sood, J. Namkoong, J. J. Martino, A. Koganti, H. Zhu, C. Robbins, I. Makalowska, S.-S. Shin, Y. Marin, K. G. Roberts, L. M. Yudt, A. Chen, J. Cheng, A. Incao, H. W. Pinkett, C. L. Graham, K. Dunn, S. M. Crespo-Carbone, K. R. Mackason, K. B. Ryan, D. Sinsimer, J. Goydos, K. R. Reuhl, M. Eckhaus, P. S. Meltzer, W. J. Pavan, J. M. Trent, S. Chen, Melanoma mouse model implicates metabotropic glutamate signaling in melanocytic neoplasia. *Nat. Genet.* **34**, 108–112 (2003).
49. M. Schäfer, S. Werner, Cancer as an overhealing wound: An old hypothesis revisited. *Nat. Rev. Mol. Cell Biol.* **9**, 628–638 (2008).
50. L. Zitvogel, L. Apetoh, F. Ghiringhelli, F. André, A. Tesniere, G. Kroemer, The anticancer immune response: Indispensable for therapeutic success? *J. Clin. Invest.* **118**, 1991–2001 (2008).

51. T. C. Gangadhar, R. H. Vonderheide, Mitigating the toxic effects of anticancer immunotherapy. *Nat. Rev. Clin. Oncol.* **11**, 91–99 (2014).
52. T. N. Schumacher, R. D. Schreiber, Neoantigens in cancer immunotherapy. *Science* **348**, 69–74 (2015).
53. C. Nardella, J. G. Clohessy, A. Alimonti, P. P. Pandolfi, Pro-senescence therapy for cancer treatment. *Nat. Rev. Cancer* **11**, 503–511 (2011).
54. W. W. Overwijk, M. R. Theoret, S. E. Finkelstein, D. R. Surman, L. A. de Jong, F. A. Vyth-Dreese, T. A. Dellemijn, P. A. Antony, P. J. Spiess, D. C. Palmer, D. M. Heimann, C. A. Klebanoff, Z. Yu, L. N. Hwang, L. Feigenbaum, A. M. Kruisbeek, S. A. Rosenberg, N. P. Restifo, Tumor regression and autoimmunity after reversal of a functionally tolerant state of self-reactive $CD8^+$ T cells. *J. Exp. Med.* **198**, 569–580 (2003).
55. K. A. Hogquist, S. C. Jameson, W. R. Heath, J. L. Howard, M. J. Bevan, F. R. Carbone, T cell receptor antagonist peptides induce positive selection. *Cell* **76**, 17–27 (1994).
56. T. Yamazaki, H. Akiba, H. Iwai, H. Matsuda, M. Aoki, Y. Tanno, T. Shin, H. Tsuchiya, D. M. Pardoll, K. Okumura, M. Azuma, H. Yagita, Expression of programmed death 1 ligands by murine T cells and APC. *J. Immunol.* **169**, 5538–5545 (2002).
57. Y. Agata, A. Kawasaki, H. Nishimura, Y. Ishida, T. Tsubat, H. Yagita, T. Honjo, Expression of the PD-1 antigen on the surface of stimulated mouse T and B lymphocytes. *Int. Immunol.* **8**, 765–772 (1996).
58. F. Tsushima, H. Iwai, N. Otsuki, M. Abe, S. Hirose, T. Yamazaki, H. Akiba, H. Yagita, Y. Takahashi, K. Omura, K. Okumura, M. Azuma, Preferential contribution of B7-H1 to programmed death-1-mediated regulation of hapten-specific allergic inflammatory responses. *Eur. J. Immunol.* **33**, 2773–2782 (2003).
59. B. Baban, A. Hansen, P. Chandler, A. Manlapat, A. Bingaman, D. Kahler, D. Munn, A. Mellor, A minor population of splenic dendritic cells expressing CD19 mediates IDO-dependent T cell suppression via type I interferon-signaling following B7 ligation. *Int. Immunol.* **17**, 909–919 (2005).
60. A. L. Mellor, B. Baban, P. Chandler, B. Marshall, K. Jhaver, A. Hansen, P. A. Koni, M. Iwashima, D. H. Munn, Cutting edge: Induced indoleamine 2,3 dioxygenase expression in dendritic cell subsets suppresses T cell clonal expansion. *J. Immunol.* **171**, 1652–1655 (2003).
61. J. D. Fontenot, J. P. Rasmussen, L. M. Williams, J. L. Dooley, A. G. Farr, A. Y. Rudensky, Regulatory T cell lineage specification by the forkhead transcription factor Foxp3. *Immunity* **22**, 329–341 (2005).
62. M. L. Bettini, F. Pan, M. Bettini, D. Finkelstein, J. E. Rehg, S. Floess, B. D. Bell, S. F. Ziegler, J. Huehn, D. M. Pardoll, D. A. A. Vignali, Loss of epigenetic modification driven by the Foxp3 transcription factor leads to regulatory T cell insufficiency. *Immunity* **36**, 717–730 (2012).
63. J. M. Kim, J. P. Rasmussen, A. Y. Rudensky, Regulatory T cells prevent catastrophic autoimmunity throughout the lifespan of mice. *Nat. Immunol.* **8**, 191–197 (2007).
64. X. Zhou, S. L. Bailey-Bucktrout, L. T. Jeker, C. Penaranda, M. Martinez-Llordella, M. Ashby, M. Nakayama, W. Rosenthal, J. A. Bluestone, Instability of the transcription factor Foxp3 leads to the generation of pathogenic memory T cells in vivo. *Nat. Immunol.* **10**, 1000–1007 (2009).
65. D. H. Castrillon, L. Miao, R. Kollipara, J. W. Horner, R. A. DePinho, Suppression of ovarian follicle activation in mice by the transcription factor Foxo3a. *Science* **301**, 215–218 (2003).
66. M. M. McFarland-Mancini, H. M. Funk, A. M. Paluch, M. Zhou, P. V. Giridhar, C. A. Mercer, S. C. Kozma, A. F. Drew, Differences in wound healing in mice with deficiency of IL-6 versus IL-6 receptor. *J. Immunol.* **184**, 7219–7228 (2010).
67. L. D. Falo Jr., M. Kovacsovics-Bankowski, K. Thompson, K. L. Rock, Targeting antigen into the phagocytic pathway in vivo induces protective tumour immunity. *Nat. Med.* **1**, 649–653 (1995).
68. R. S. Chu, O. S. Targoni, A. M. Krieg, P. V. Lehmann, C. V. Harding, CpG oligodeoxynucleotides act as adjuvants that switch on T helper 1 (Th1) immunity. *J. Exp. Med.* **186**, 1623–1631 (1997).

Acknowledgments: We thank J. G. Clohessy (Harvard Medical School) for advice on dosing of VO-OHpic, S. Chen (Rutgers University) for the gift of Tg(*Grm1*)Epv mice, and M. Azuma for the gift of anti–PD-L1 mAb. **Funding:** This study was supported by NIH R01 grants CA096651, CA103320, and CA112431; the Lovick P. and Elizabeth T. Corn Foundation (to D.H.M.); R01 HL11879 and CA72669 (to B.R.B); R01 AI077610 (to J.D.P.); R01 AI083005 and AI103347 (to A.L.M.); and grant 26290059 from the Ministry of Education, Culture, Sports, Science, and Technology, Japan (to H.Y.). **Author contributions:** D.H.M. supervised the study and wrote the manuscript. M.D.S. and D.H.M. designed, performed, and interpreted all studies with tumors and apoptotic tumor cells. T.L.M., in conjunction with R.S., designed and interpreted the lupus model studies. R.S. performed and analyzed the lupus model studies. R.B.H. and J.D.W. discussed the design and interpretation of the PD-1 blocking studies. E.C. assisted with the design and interpretation of the CD8 bead studies. A.L.M., with L.H., discussed the design and interpretation of the PD-1 and IDO studies. M.R.M. provided reagents and discussed the interpretation of the IDO studies. A.H.S. and L.M.F. provided PD-1 and PD-L1/2 knockout mice. H.Y. provided blocking antibodies. J.D.P. participated in the design and interpretation of the mTOR studies. B.R.B. participated in the design of the PD-1, IDO, and mTOR studies and discussed results. B.R.B., A.H.S., J.D.P., M.R.M., E.C., and A.L.M. provided critical comments on, discussed, and helped revise the manuscript. **Competing interests:** D.H.M., A.L.M., and B.R.B. have intellectual property interests in the therapeutic use of IDO inhibitors. D.H.M. and A.L.M. receive consulting income and research support from NewLink Genetics Inc. **Data and materials availability:** All data needed to evaluate the conclusions in the paper are present in the paper and/or the Supplementary Materials. Additional data related to this paper may be requested from the authors.

Submitted 25 June 2015
Accepted 14 August 2015
Published 6 November 2015
10.1126/sciadv.1500845

Citation: M. D. Sharma, R. Shinde, T. L. McGaha, L. Huang, R. B. Holmgaard, J. D. Wolchok, M. R. Mautino, E. Celis, A. H. Sharpe, L. M. Francisco, J. D. Powell, H. Yagita, A. L. Mellor, B. R. Blazar, D. H. Munn, The PTEN pathway in T_{regs} is a critical driver of the suppressive tumor microenvironment. *Sci. Adv.* **1**, e1500845 (2015).